Chemical Geology 271 (2010) 70–85

Contents lists available at ScienceDirect

Chemical Geology

journal homepage: www.elsevier.com/locate/chemgeo

# Chemical variations and regional diversity observed in MORB

Ricardo Arevalo Jr. *, William F. McDonough

*Department of Geology, University of Maryland, College Park, MD, 20742, USA*

ARTICLE INFO

*Article history:*
Received 14 April 2009
Received in revised form 4 December 2009
Accepted 17 December 2009

Editor: D.B. Dingwell

*Keywords:*
MORB
DMM
Basalt
Trace element
Concentration ratio

ABSTRACT

An assemblage of MORB analyses ($n=792$ samples), including a suite of new, high-precision LA-ICP-MS measurements ($n=79$), has been critically compiled in order to provide a window into the chemical composition of these mantle-derived materials and their respective source region(s), commonly referred to as the depleted MORB mantle (DMM). This comprehensive MORB data set, which includes both "normal-type" (N-MORB, defined by $(La/Sm)_N<1.00$) and "enriched-type" samples (E-MORB, $(La/Sm)_N\geq 1.00$), defines a global MORB composition that is more enriched in incompatible elements than previous models. A statistical evaluation of the true constancy of "canonical" trace element ratios using this data set reveals that during MORB genesis Ti/Eu, Y/Ho and Ce/Pb remain constant at the 95% confidence-level; thus, the ratios recorded in MORB ($Ti/Eu=7060\pm1270$, $2\sigma$; $Y/Ho=28.4\pm3.6$, $2\sigma$; $Ce/Pb=22.2\pm9.7$, $2\sigma$) may reflect the composition of the DMM, presuming the degree of source heterogeneity, component mixing and conditions of melting/crystallization of the DMM are adequately recorded by global MORB. Conversely, Ba/Th, Nb/U, Zr/Hf, Nb/Ta, Sr/Nd, and Th/U are shown to fractionate as a function of MORB genesis, and thus these ratios do not faithfully record the composition of the DMM.

Compared to samples from the Pacific and Indian Oceans, MORB derived from Atlantic ridge segments are characterized by statistically significant (≥95% confidence-level) enrichments in both highly incompatible elements (e.g., light REE, TITAN group elements, Sr, Ba, Pb, Th, and U) as well as less incompatible elements (e.g., heavy REE), indicating: i) a prominent recycled source component; ii) variable proportions of pyroxenite in the Atlantic source region; and/or, most likely iii) smaller degrees of melting and/or greater extents of fractional crystallization due to slower ridge spreading rates. Conversely, Pacific MORB has the most depleted regional signatures with regard to highly incompatible elements (e.g., Ba, Pb, Th, and U), likely due to faster ridge spreading rates. Indian Ocean MORB exhibit limited variation in incompatible element enrichments/depletions but are generally the most depleted in more compatible elements (e.g., Ti, Cr, Sc, and heavy REE), potentially due to distinct source characteristics or deep source melting in the garnet field. Atlantic, Pacific and Indian MORB can also be distinguished by trace element ratios, particularly Ce/Pb and Th/U, which is distinct at the >99% confidence-level. Global MORB, and by inference the DMM, are characterized by enrichments in Y/Ho and depletions in Th/U relative to the chondritic ratios, and are complementary to the continental crust. However, the median of global MORB and the bulk continental crust both have sub-chondritic Ti/Eu and Nb/Ta ratios, suggesting an under-represented Ti- and Nb-rich reservoir in the Earth, potentially refractory, rutile-bearing eclogite at depth in the mantle.



## 1. Introduction

The chemical compositions of the individual components that constitute the silicate Earth (SE), including the largely depleted source of mid-ocean ridge basalts (MORB), the enriched mantle domain(s) frequently observed in ocean island basalts (OIB), and the incompatible element-rich continental crust, are important parameters for models of oceanic and continental crust generation, subduction and crustal recycling, mantle source mixing, intraplate volcanism, island arc processes, and the thermal evolution of the planet. As opposed to major element compositions, which exhibit limited diversity and primarily reflect the source lithology, trace element abundances span orders of magnitude and provide a perspective into mantle processes as well as source compositions because mantle phases incorporate and exclude trace elements with much greater selectivity than major elements. Thus, trace elements hold the key to understanding the evolution of the SE and its major source reservoirs.

The chemical and isotopic compositions of mantle derivatives, such as MORB, OIB and island arc volcanics, reflect the compositions of their respective source regions but also the extent of mixing between different source components, degree of melting and/or fractional crystallization (Stracke and Bourdon, 2009), in addition to the tectonic

* Corresponding author. Tel.: +1 301 405 6248; fax: +1 301 405 3597.
*E-mail address:* gatorick@umd.edu (R. Arevalo).

0009-2541/$ – see front matter © 2009 Elsevier B.V. All rights reserved.
doi:10.1016/j.chemgeo.2009.12.013

environment, crustal contamination and potential post-eruptive alteration. Mid-ocean ridge basalts, which are predominantly tholeiitic in composition (e.g., Engel et al., 1965; Melson et al., 1976), provide an ideal case study of the modern mantle as these melts represent adiabatic upwelling and decompression of the ambient upper mantle (e.g., McKenzie and O'Nions, 1991), and therefore these samples exemplify a relatively simple melting history. Additionally, the average global rate of magma emplacement is between about 26 and 34 $km^3\ yr^{-1}$, of which 75% is generated by mid-ocean ridge volcanism (Crisp, 1984); thus, MORB samples are generally fresh (<1 Ma), abundant and accessible. The MORB source region, or depleted MORB mantle (DMM), is largely depleted in incompatible trace elements ($D_i^{sol/liq}<1$), those elements that preferentially partition into melt phases over residual solids, relative to more compatible trace elements. The depleted composition of the DMM has long been identified as a complementary geochemical signature compared with the incompatible element enriched continental crust (e.g., Hofmann, 1988; Sun and McDonough, 1989), with several notable exceptions (e.g., Nb and Ta; McDonough, 1990).

Multiple studies have attempted to constrain the chemical composition of the DMM, including models based on upper mantle melts (i.e., MORB; Salters and Stracke, 2004) and residues (i.e., abyssal peridotites; Workman and Hart, 2005), as well as inferences based on cosmochemical arguments (i.e., super-chondritic $^{142}Nd/^{144}Nd$ observed in terrestrial samples; Boyet and Carlson, 2006); however, the absolute depletion of this mantle volume remains unsettled due to difficulties in modeling the incompatible element budget of the DMM, which is a consequence of the wide variance in incompatible element concentrations observed in MORB and off-axis seamounts (e.g., Zindler et al., 1984; Graham et al., 1988; Hofmann, 1988; Sun and McDonough, 1989; Graham et al., 1996; Niu and Batiza, 1997; Hofmann, 2003), as well as upper mantle peridotites and xenoliths (e.g., Jagoutz et al., 1979; Nixon et al., 1981; McDonough and Frey, 1989; McDonough and Sun, 1995; Niu, 2004).

Trace element concentrations in MORB provide one way to constrain the composition of the DMM, as these mantle derivatives generally represent mafic melts of their source. Highly incompatible elements, though, commonly show skewed frequency distributions in terrestrial samples (Ahrens, 1954; McDonough, 1990) and thus pose a challenge to interpreting the representative trace element chemistry of global MORB. In oceanic basalts, canonical trace element ratios such as Zr/Hf, Ce/Pb, Nb/Ta, and Th/U have also been used to characterize mantle sources (e.g., Jochum et al., 1983; Hofmann et al., 1986, Newsom et al., 1986; Hofmann, 1988; Sun and McDonough, 1989; Salters and Stracke, 2004; Workman and Hart, 2005; Boyet and Carlson, 2006). However, the utility of these ratios hinges on the presumption of equivalent partitioning behavior during MORB genesis and the assumption that source heterogeneity, component mixing and variations in melting/crystallization conditions are adequately represented by the melts (Stracke and Bourdon, 2009).

Here, we report new high-precision, externally calibrated trace element measurements of a global suite of MORB and incorporate these data into a critically compiled database that includes other high-quality analyses from several recently published, peer-reviewed data sets. With this comprehensive database we attempt to: i) establish a representative composition for global MORB; ii) investigate potential influences of mantle source mixing (which may affect the distribution of trace elements in MORB); iii) statistically evaluate the effects of fractional melting and the preservation of canonical trace element ratios during MORB genesis; and, iv) identify prospective geochemical distinctions between MORB samples derived from the Atlantic, Pacific and Indian Ocean basins.

## 2. Global MORB database

Our new trace element concentration data were determined via high-precision laser ablation (LA-) ICP-MS methods and include analyses of both depleted and enriched MORB endmembers. Following the protocol established by Arevalo and McDonough (2008), external calibration techniques were implemented in order to maximize precision and accuracy as well as account for any potential non-spectral matrix effects; two USGS basaltic glasses (BIR-1G and BCR-2G; c.f., Jochum et al., 2005a) and five MPI-DING silicate glasses (BM90/21-G, ML3B-G, StHs6/80-G, KL2-G, and T1-G; c.f., Jochum et al., 2000, 2005b), which together span between $10^{0.5}$ and $10^{3.1}$ orders of magnitude in concentration for all elements measured here, were used as standard reference materials for external calibration (see Supplemental materials). Spectral matrix effects, particularly isobaric interferences from potential diatomic oxides, were limited by implementing a standard tuning procedure that maximized the elemental signal (based on $^{43}Ca$ and $^{232}Th$ spectra) and minimized oxide production ($^{232}Th^{16}O/^{232}Th \leq 0.15\%$). The typical external reproducibility for our concentration measurements, which include new data for Sc, Cr, Sr, Y, Zr, Nb, Ba, the rare-earth elements (REE; from La to Lu), Hf, Ta, and Pb were determined to be $\leq 3\%$ ($2\sigma_m$) for four replicate analyses of each sample. The abundances of P, K, Ti, W, Th, and U were originally reported by Arevalo and McDonough (2008) and Arevalo et al. (2009).

A comprehensive collection of trace element data for a more complete global set of MORB was manually compiled from a number of reliable references with established, high-precision and demonstrably accurate methods of analysis (c.f., replicate measurements of standard reference materials, such as BCR-1, BHVO-1 and VG-2) in order to complement the new MORB data presented here. The inclusive data set ($n=792$ samples), which encompasses a wide geographic distribution (Fig. 1) and includes samples from the Atlantic ($n=342$), Pacific ($n=259$) and Indian ($n=191$) Oceans, also consist of: i) LA-ICP-MS trace element measurements for a global spectrum of MORB reported by Sun et al. (2003, 2008); ii) the PetDB MORB data set from Salters and Stracke (2004), which was filtered to include only samples with <55 wt. % $SiO_2$, smooth REE patterns and eruption depths in excess of 2000 m; iii) ICP-MS, isotope dilution (ID-) thermal ionization mass spectrometry (TIMS) and ID-ICP-MS measurements of MORB samples from the Gorda Ridge (Davis et al., 2008) and on-axis (Sims et al., 2002; Hall et al., 2006) and off-axis lavas from the East Pacific Rise (Sims et al., 2003); and, iv) Indian MORB analyses from Mahoney et al. (2002), Janney et al. (2005) and Nauret et al. (2006), which comprise measurements of dissolved sample solutions via ICP-MS and ID-ICP-MS. An Excel spreadsheet with the compiled data set, including the new data reported here, can be accessed in the Supplemental materials.

## 3. The definition and chemical composition of prototypical MORB

### 3.1. Normal- versus enriched-type MORB

Mid-ocean ridge basalts, which represent mafic melts of a mantle reservoir that has largely been depleted due to the extraction of the continental crust early in Earth's history (e.g., Hofmann, 1988; Sun and McDonough, 1989), are mostly unaffected by contamination by the continental crust and are highly variable in composition, particularly with regard to incompatible trace elements (those that concentrate in the liquid, i.e., MORB, over the solid, i.e., residual mantle peridotite). As far back as the work of Schilling (1973), MORB have often been subdivided into two distinct categories: "normal-type" and "enriched-type" samples. Normal-type MORB, or N-MORB, represent the majority of global MORB samples and are characterized by depletions in highly incompatible elements (e.g., large-ion lithophile elements, LILE, and high-field strength elements, HFSE) relative to more compatible elements (e.g., Engel et al., 1965; Melson et al., 1976; Hofmann, 1988; Sun and McDonough, 1989; Hofmann, 2003 and references therein), resulting in diagnostic trace element ratios (e.g., $(La/Sm)_N<1$) and isotopic compositions (e.g., high εNd and low $^{87}Sr/^{86}Sr$). Alternatively, enriched-type MORB, or E-MORB, represent a subordinate component of global MORB and are anomalously enriched in

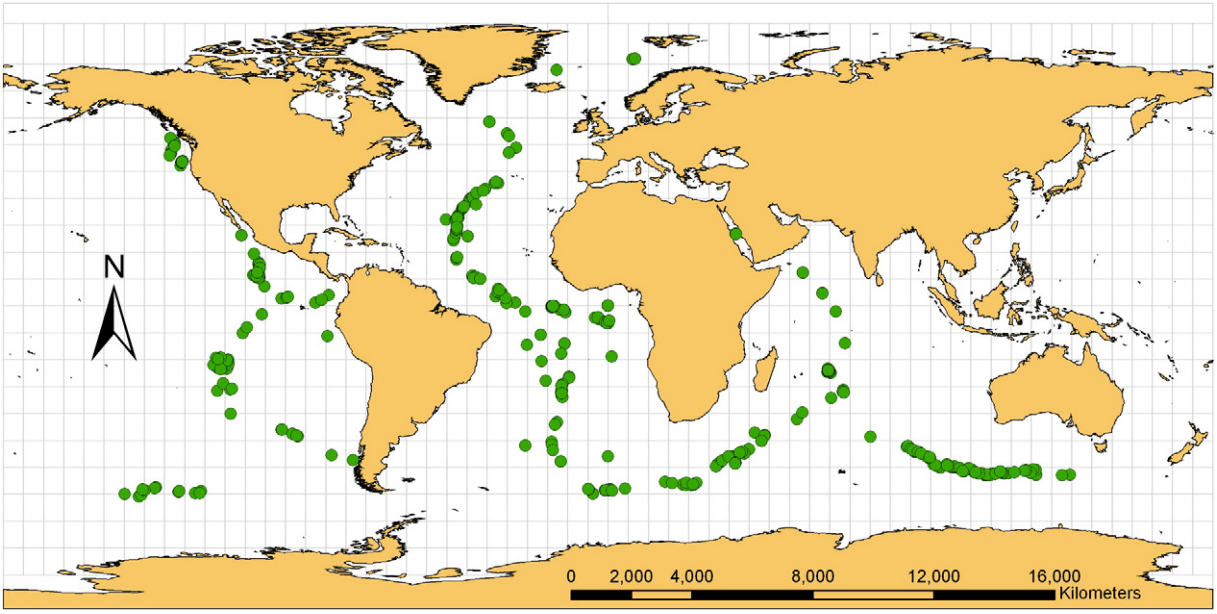


**Fig. 1.** Geographic distribution of the global MORB samples ($n=792$) analyzed and/or manually compiled here.

highly incompatible elements, resulting in trace element ratios and isotopic compositions (e.g., $(La/Sm)_N \geq 1$, low εNd and high $^{87}Sr/^{86}Sr$) distinct from more common N-MORB. Although segments of the East Pacific Rise have been documented to yield up to 5–10% E-MORB (Langmuir et al., 1986; Lundstrom et al., 1999), Donnelly et al. (2004) estimate that ≤3% of MORB are chemically enriched based on: i) the frequency distribution of N- and E-MORB sampled at the Mid-Atlantic Ridge south of the Kane zone (MARK area), a spreading region far from any known mantle hotspot; and, ii) a two-stage melting model of E-MORB genesis, involving metasomatism of ambient mantle peridotite by low-degree melts (i.e., $F<0.01$) of peridotite or eclogite, followed by typical MORB melting (i.e., $F\approx 0.10$) of the newly enriched mantle source.

The origin of the enriched geochemical signatures observed in E-MORB relative to the depleted signatures characteristic of N-MORB has long been suspected to represent the infiltration of undepleted or enriched lower mantle materials into the ambient (depleted) upper mantle (e.g., Schilling, 1973; Schilling et al., 1983; Allègre et al., 1984; le Roex et al., 1985; Schilling, 1991; Taylor et al., 1997), though metasomatism of ambient upper mantle peridotite by low-degree partial melts (e.g., Sun and Hanson, 1975; Wood, 1979; Allègre and Turcotte, 1986; Sun and McDonough, 1989; Niu et al., 1996; Donnelly et al., 2004) and/or melting of enriched eclogitic domains derived from subducted oceanic crust (e.g., Hofmann and White, 1982; Allègre et al., 1984; Zindler et al., 1984; Niu and Batiza, 1997; Niu et al., 1999) have also been suggested. Regardless of the exact origin of the source materials that contribute to the genesis of E-MORB, several filters (primarily La/Sm, $(La/Sm)_N$ and K/Ti ratios) can be and have been implemented to distinguish between N- and E-MORB.

Because collections of MORB do not represent a perfectly random sampling of the entire mid-ocean ridge system, the division of MORB samples into normal- and enriched-types has traditionally served as a way to avoid over-representing enriched samples when characterizing the global MORB reservoir, and by inference geochemical models of the DMM and bulk SE. However, the global spectrum of MORB exhibits a continuous range in compositions, from highly depleted to enriched in incompatible element abundances (e.g., Hofmann, 2003 and references therein), and thus dividing samples based upon an arbitrary chemical criterion also serves to bias models of global MORB. As a result, here we establish a representative composition of global MORB, as represented by both normal and enriched endmembers. Anomalous samples with La/Sm ratios outside of the "outer fence," or 3× the interquartile range of values in this inclusive data set, are considered statistical outliers and are not considered here (see Supplemental materials). For comparison, we also examine the composition of only N-MORB, defined here as samples with $(La/Sm)_N<1.00$ ($n=597$ out of 792 total MORB samples), in order to evaluate and quantify the effects of enriched mantle components in the DMM.

### 3.2. The chemical composition of global MORB and N-MORB

Frequency distributions of highly incompatible trace elements (e.g., Ba, Th, U, and the light REE) in the MORB compilation examined here show ranges in concentrations that span nearly three orders of magnitude and are positively skewed rather than Gaussian, or "bell-shaped," in geometry (Fig. 2). As first recognized by Ahrens (1954), such skewed distributions may be anticipated for incompatible element abundances in terrestrial samples and can be converted into normal

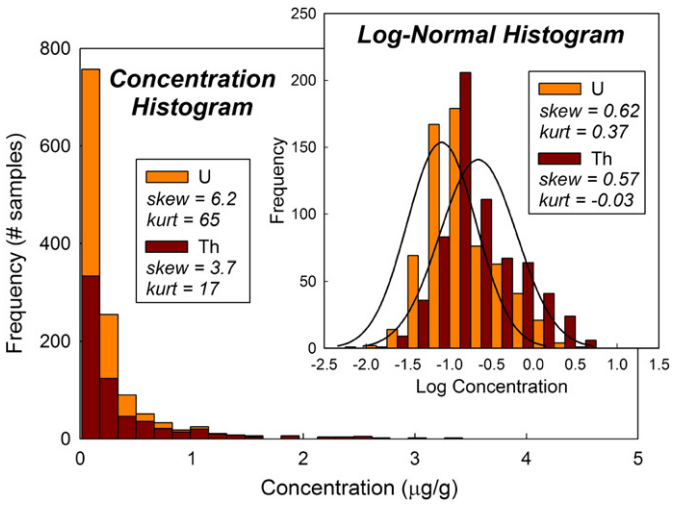


**Fig. 2.** Examples of frequency distributions of highly incompatible trace element abundances in global MORB. Both Th and U are highly incompatible during mantle melting and thus are characterized by skewed distributions; however, taking the logarithm of the sample abundances of these elements normalizes the data into distributions with a more Gaussian geometry (Ahrens, 1954).

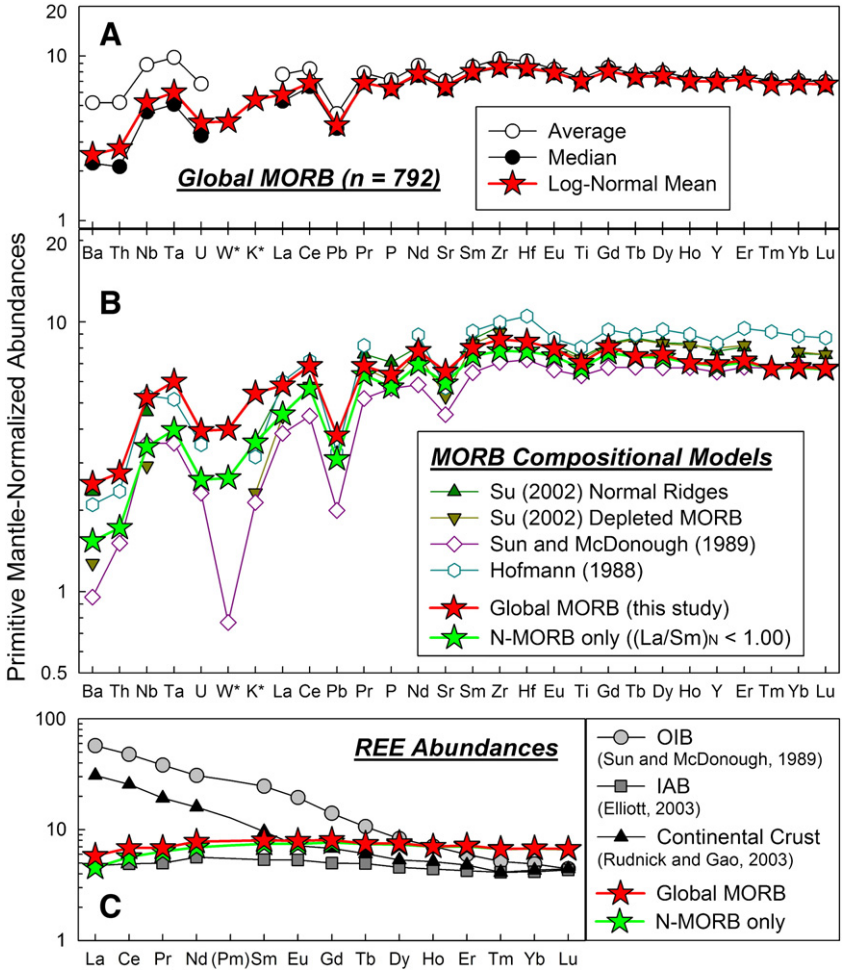


**Fig. 3.** Primitive-mantle normalized abundances of trace elements in various compositional models of MORB chemistry. The elements along the abscissa are ordered by relative incompatibilities observed in MORB, as determined in previous studies (e.g., Hofmann, 1988; Sun and McDonough, 1989) and here. (A) The log-normal mean abundances of trace elements in our global MORB data set mimic the median rather than the statistical average due to the skewed frequency distributions of highly incompatible elements observed in terrestrial samples (see Fig. 2). (B) Global MORB represent a more incompatible element enriched composition compared to N-MORB and previous models of MORB composition, though the abundances of the less incompatible heavy REE merge with the values observed in N-MORB and predicted by Sun and McDonough (1989). (C) Although the abundances of light REE in global and N-MORB are depleted similar to typical IAB (as modeled by Elliott, 2003), the heavy REE observed in MORB are actually enriched relative to IAB, OIB and the bulk continental crust.

distributions by simply taking the logarithm of the variate, or the elemental concentration. Distributions of logarithmic concentrations are generally Gaussian in character (Fig. 2), and thus allow a statistical analysis of the mean concentration of both highly incompatible and moderately incompatible elements in MORB. Comparisons of the average and median values with the log-normal mean values for the chemical composition of global MORB and N-MORB are illustrated in Fig. 3; the log-normal mean values approximate the median (as expected for a skewed sample populations; e.g., McDonough, 1990). The average, median and log-normal mean values all converge towards the less incompatible elements (e.g., heavy REE).

Table 1 defines the incompatible element budget of both global MORB and N-MORB as determined by the log-normal distribution of elements in the data set compiled here. Samples with anomalous trace element abundances that have been diagnosed as statistical outliers, defined by concentrations that reside outside of the "outer fence," or 3× the interquartile range, were not considered in our analytical investigations. The global MORB and N-MORB model compositions established here, which have 7.84 wt.% and 8.01 wt.% MgO respectively, are compared to previous characterizations of MORB based on trace element abundances measured in independent sample sets (Hofmann, 1988; Su, 2002) and an early survey of literature values (Sun and McDonough, 1989). Fig. 3 illustrates the similarities and differences between the trace element patterns exhibited by each model composition. Whereas the model of Sun and McDonough (1989) delineates the most incompatible element depleted model composition of MORB, the log-normal mean composition of global MORB, as determined here, represents the most enriched composition. The highest abundances of the heavy REE, however, are modeled by Hofmann (1988).

The complete chemical composition of global MORB, including major, minor and volatile elements, is expounded in Table 2, which compares the chemistry of MORB to CI carbonaceous chondrites, as surveyed by Palme and Jones (2003), and the unfractionated SE, as modeled primarily by McDonough and Sun (1995). The major element chemistry of global MORB has been derived from the median composition of the global data set presented here, whereas minor elements (e.g., first-row transition metals), trace elements not reported here (e.g., platinum-group elements) and volatile species (e.g., halogens) have been derived through other analytical proxies defined in Table 2.

## 4. Relative incompatibilities during MORB genesis

### 4.1. MORB melting models

The simplest model of upper mantle melting at mid-ocean ridges assumes passive upwelling and decompression-induced melting as

**Table 1**
Incompatible element budget (in μg/g) of global MORB compared to N-MORB and previous model compositions.

| Element | Global MORB[a] average | Standard Deviation | Skewness | *n* | Median | Global MORB[a] log-normal mean | N-MORB only[b] log-normal mean | Su (2002) Normal segments[c] | Su (2002) Depleted samples[d] | Sun and McDonough (1989) N-MORB[e] | Hofmann (1988) N-MORB[f] |
|---|---|---|---|---|---|---|---|---|---|---|---|
| P[g] | 641 | 371 | 2.7 | 695 | 567 | 574 | 515 | 637 | 546 | 510 | |
| K[h] | – | – | – | – | – | 1520 | 1000 | 1030 | 650 | 600 | 884 |
| Sc | 37.0 | 4.9 | −0.9 | 502 | 37.2 | 36.8 | 37.8 | | | | 41 |
| Ti | 8820 | 2520 | 1.4 | 679 | 8350 | 8500 | 8100 | 8930 | 8750 | 7600 | 9682 |
| Cr | 326 | 91 | 0.7 | 219 | 321 | 326 | 330 | | | | |
| Sr | 140 | 59 | 3.3 | 674 | 125 | 130 | 118 | 122 | 105 | 90 | 113 |
| Y | 31.4 | 10.2 | 5.5 | 654 | 30.0 | 30.0 | 29.6 | 33.5 | 34.4 | 28.0 | 35.8 |
| Zr | 100 | 55 | 4.0 | 655 | 89.1 | 90.1 | 81.6 | 101 | 95.2 | 74.0 | 104 |
| Nb | 5.82 | 7.6 | 3.0 | 651 | 3.00 | 3.44 | 2.27 | 3.05 | 1.92 | 2.33 | 3.51 |
| Ba | 34.2 | 49.0 | 2.7 | 684 | 14.7 | 16.6 | 10.2 | 15.5 | 8.40 | 6.30 | 13.9 |
| La | 5.00 | 4.99 | 3.4 | 754 | 3.44 | 3.77 | 2.94 | 3.70 | 2.90 | 2.50 | 3.90 |
| Ce | 14.0 | 11.1 | 3.3 | 723 | 10.9 | 11.5 | 9.49 | 11.6 | 9.65 | 7.50 | 12.0 |
| Pr | 2.00 | 1.27 | 4.4 | 378 | 1.75 | 1.74 | 1.62 | 1.93 | 1.71 | 1.32 | 2.07 |
| Nd | 10.9 | 6.1 | 3.3 | 723 | 9.49 | 9.8 | 8.67 | 10.1 | 9.50 | 7.30 | 11.2 |
| Sm | 3.49 | 1.46 | 3.3 | 754 | 3.19 | 3.25 | 3.03 | 3.50 | 3.37 | 2.63 | 3.75 |
| Eu | 1.28 | 0.40 | 2.3 | 731 | 1.21 | 1.22 | 1.15 | 1.27 | 1.23 | 1.02 | 1.34 |
| Gd | 4.64 | 1.67 | 3.6 | 619 | 4.43 | 4.40 | 4.17 | 4.52 | 4.48 | 3.68 | 5.08 |
| Tb | 0.763 | 0.209 | 3.1 | 438 | 0.730 | 0.738 | 0.733 | 0.860 | 0.850 | 0.670 | 0.885 |
| Dy | 5.33 | 1.71 | 4.5 | 649 | 5.04 | 5.11 | 4.97 | 5.64 | 5.60 | 4.55 | 6.30 |
| Ho | 1.11 | 0.41 | 6.0 | 370 | 1.05 | 1.05 | 1.05 | 1.24 | 1.22 | 1.01 | 1.34 |
| Er | 3.29 | 1.09 | 6.0 | 647 | 3.16 | 3.15 | 3.10 | 3.53 | 3.58 | 2.97 | 4.14 |
| Tm | 0.481 | 0.196 | 6.3 | 309 | 0.460 | 0.453 | 0.454 | | | 0.456 | 0.621 |
| Yb | 3.12 | 1.05 | 7.1 | 728 | 3.00 | 3.00 | 2.97 | 3.36 | 3.41 | 3.05 | 3.90 |
| Lu | 0.471 | 0.158 | 6.9 | 706 | 0.45 | 0.454 | 0.450 | 0.510 | 0.510 | 0.455 | 0.589 |
| Hf | 2.64 | 1.38 | 4.5 | 673 | 2.35 | 2.40 | 2.20 | | | 2.05 | 2.97 |
| Ta | 0.364 | 0.449 | 2.7 | 562 | 0.189 | 0.224 | 0.148 | | | 0.132 | 0.192 |
| W[i] | – | – | – | – | – | 0.052 | 0.034 | | | 0.010 | |
| Pb | 0.668 | 0.467 | 3.2 | 603 | 0.544 | 0.570 | 0.465 | | | 0.300 | 0.489 |
| Th | 0.415 | 0.630 | 3.7 | 648 | 0.169 | 0.219 | 0.137 | | | 0.120 | 0.187 |
| U | 0.137 | 0.213 | 6.2 | 638 | 0.066 | 0.080 | 0.053 | | | 0.047 | 0.071 |

[a] Statistical outliers plotting outside of the "outer fence," defined by 3× the interquartile range, were not considered.
[b] Log-normal mean abundances in MORB with $(La/Sm)_N<1.00$.
[c] Compositional model based on weighting MORB analyses according to 151 ridge segments located away from subduction zones or known hotspots.
[d] Compositional model based on weighting MORB analyses according to 62 normal ridge segments with average $K_2O/TiO_2<0.067$.
[e] Early survey of literature values of MORB characterized by depletions in light REE.
[f] Average composition of 26 MORB glasses characterized by depletions in light REE.
[g] P abundances converted from $P_2O_5$ major element analyses.
[h] Global MORB and N-MORB K abundances calculated assuming a global MORB K/U = 19,000 and an N-MORB K/U = 20,000 after Arevalo et al. (2009).
[i] Global MORB and N-MORB W abundances calculated assuming a silicate Earth W/U = 0.65 after Arevalo and McDonough (2008).

approximated as a reversible, adiabatic process with isentropic productivity (e.g., Asimow et al., 1997 and references therein). If a mantle melt remains in contact with the residue during magma migration and emplacement, then the bulk composition of the system (melt + residue) is effectively held constant and the melting process may be approximated by equilibrium (or batch) melting (e.g., Kinzler and Grove, 1992). However, realistic models of melt generation and segregation implicate polybaric near-fractional melting rather than equilibrium melting at mid-ocean ridges (Langmuir et al., 1977; Wood et al., 1979a, 1979b; McKenzie, 1984; McKenzie and Bickle, 1988; Johnson et al., 1990; Spiegelman and Kenyon, 1992; Hart, 1993; Iwamori, 1993; Sobolev and Shimizu 1993; Kelemen et al., 1997). Additionally, U-series disequilibria in global MORB robustly demonstrate that the isotopic composition of most MORB cannot be reproduced via equilibrium melting models without requiring unrealistically small degrees of melting, but require near-fractional melting and/or more complex melting mechanisms (e.g., Condomines et al., 1981; Newman et al., 1983; McKenzie, 1985; Goldstein et al., 1989, 1992; Rubin and MacDougall, 1992; Goldstein et al., 1993; Volpe and Goldstein, 1993; Sims et al., 1995).

Consequently, here we adapt a simplified model of (modal) accumulated fractional melting following Shaw (1970), where the concentration of element $i$ in a mantle melt ($C_i^{liq}$), such as MORB, is related to the concentration in the source ($C_i^0$), such as the DMM, in addition to the degree of partial melting ($F$) and the partition coefficient ($D_i^{sol/liq}$):

$$C_i^{liq} = \frac{C_i^0}{F}\left(1-(1-F)^{1/D_i^{sol/liq}}\right). \quad (1)$$

Here it may be seen that incompatible trace elements ($D_i^{sol/liq}<1$) concentrate in the liquid, particularly at low degrees of melting ($F$). Following this model, the concentration ratio of two elements $i$ and $j$ in MORB is given by:

$$\frac{C_i^{MORB}}{C_j^{MORB}} = \left(\frac{C_i^{DMM}}{C_j^{DMM}}\right)\frac{\left(1-(1-F)^{1/D_i^{DMM/MORB}}\right)}{\left(1-(1-F)^{1/D_j^{DMM/MORB}}\right)}. \quad (2)$$

Accordingly, a concentration ratio between two trace elements may remain constant through MORB genesis under three conditions: i) if the two elements behave similarly during mantle melting (i.e., $D_i^{sol/liq}\approx D_j^{sol/liq}$); ii) if the two elements are both highly incompatible ($D_{i,j}^{sol/liq}<<1$); and/or, iii) if the system experiences unrealistically high melt fractions (i.e., $F\approx 1$). If any of these criteria is met, Eq. (3) reduces to:

$$\frac{C_i^{MORB}}{C_j^{MORB}} \approx \left(\frac{C_i^{DMM}}{C_j^{DMM}}\right) \quad (3)$$

and the ratio measured in MORB may be inferred to be representative of the source region, or local DMM, presuming the melt adequately represents the heterogeneity and contribution of all source components involved (Stracke and Bourdon, 2009).

**Table 2**
Chemical composition of global MORB.

| Element | | Cl[a] | SE[b] | MORB | Constraint | Reference(s) |
|---|---|---|---|---|---|---|
| H | μg/g | 20,200 | 120[c] | 230 | $H_2O/Ce = 180$ | Michael (1995); Saal et al. (2002); le Roux et al. (2006) |
| He | mol/g | – | – | $5.4\times10^{-10}$ | molar $C/He = 2.9\times10^{4}$ | Javoy and Pineau (1991) |
| Li | μg/g | 1.49 | 1.6 | 5.1 | Li/Yb = 1.7 | Ryan and Langmuir (1987) |
| Be | μg/g | 0.025 | 0.068 | 0.49 | Be/Nd = 0.05 | Ryan and Langmuir (1988) |
| B | μg/g | 0.69 | 0.3 | 1.5 | B/K = 0.0010 | Ryan and Langmuir (1993) |
| C | μg/g | 32,200 | 120 | 190 | $CO_2/Nb = 200$ | Saal et al. (2002); le Roux et al. (2006) |
| N | μg/g | 3180 | 2 | 0.55 | molar C/N = 400 | Javoy and Pineau (1991); Marty and Zimmermann (1999) |
| F | μg/g | 58.2 | 25 | 170 | F/P = 0.3 | Schilling et al. (1980); Saal et al. (2002) |
| Ne | mol/g | – | – | $2.1\times10^{-14}$ | molar $He/Ne = 2.6\times10^{4}$ | Sarda and Graham (1990) |
| Na | wt.% | 0.498 | 0.267 | 2.01 | Median of global MORB | This study |
| Mg | wt.% | 9.61 | 22.8 | 4.73 | Median of global MORB | This study |
| Al | wt.% | 0.849 | 2.35 | 8.19 | Median of global MORB | This study |
| Si | wt.% | 10.68 | 21 | 23.6 | Median of global MORB | This study |
| P | μg/g | 926 | 90 | 574 | Log-normal mean of global MORB | This study |
| S | μg/g | 54,100 | 250 | 1100 | S/Dy-220 | Saal et al. (2002) |
| Cl | μg/g | 698 | 17 | 140 | Cl/K-0.09 | Jambon et al. (1995); Gannoun et al. (2007) |
| Ar | mol/g | – | – | $4.2\times10^{-10}$ | molar He/Ar = 1.3 | Sarda and Graham (1990); Javoy and Pineau (1991) |
| K | μg/g | 544 | 280[d] | 1520 | Log-normal mean of global MORB | Arevalo et al. (2009) |
| Ca | wt.% | 0.932 | 2.53 | 8.23 | Median of global MORB | this study |
| Sc | μg/g | 5.9 | 16.2 | 36.8 | Log-normal mean of global MORB | This study |
| Ti | μg/g | 458 | 1200 | 8500 | Log-normal mean of global MORB | This study |
| V | μg/g | 54.3 | 82 | 250 | V/Sc = 6.7 | Lee et al. (2005) |
| Cr | μg/g | 2650 | 2620 | 326 | Log-normal mean of global MORB | This study |
| Mn | μg/g | 1930 | 1040 | 1320 | Median of global MORB | This study |
| Fe | wt.% | 18.4 | 6.26 | 7.27 | Median of global MORB | This study |
| Co | μg/g | 506 | 105 | 56 | Fe/Co = 1300 | McDonough (1994) |
| Ni | μg/g | 10,800 | 1960 | 200 | Ni/Cr = 0.6 | McDonough (1994) |
| Cu | μg/g | 131 | 30 | 70 | $Cu/Re = 8.4\times10^{4}$ | Sun et al. (2003) |
| Zn | μg/g | 323 | 55 | 80 | molar Zn/Cd = 1000 | Laul et al. (1972); Hertogen et al. (1980) |
| Ga | μg/g | 9.71 | 4.0 | 21 | molar Zn/Ga = 4.1 | Hart (1976) |
| Ge | μg/g | 32.6 | 1.1 | 1.6 | molar $Ge/Si = 2.6\times10^{-6}$ | de Argollo and Schilling (1978) |
| As | μg/g | 1.81 | 0.05 | 0.11 | $As/Ce = 9.6\times10^{-3}$ | Sims et al. (1990) |
| Se | μg/g | 21.4 | 0.075 | 0.21 | Se/Re = 250 | Hertogen et al. (1980); Morgan (1986) |
| Br | μg/g | 3.50 | 0.050 | 0.32 | Cl/Br = 430 | Jambon et al. (1995) |
| Kr | mol/g | – | – | $3.2\times10^{-16}$ | molar $He/Kr = 1.7\times10^{6}$ | Sarda and Graham (1990) |
| Rb | μg/g | 2.32 | 0.600 | 1.5 | Ba/Rb = 11 | Hofmann and White (1983) |
| Sr | μg/g | 7.26 | 19.9 | 130 | Log-normal mean of global MORB | This study |
| Y | μg/g | 1.56 | 4.3 | 30.0 | Log-normal mean of global MORB | This study |
| Zr | μg/g | 3.86 | 10.5 | 90.1 | Log-normal mean of global MORB | This study |
| Nb | ng/g | 247 | 658 | 3440 | Log-normal mean of global MORB | This study |
| Mo | ng/g | 928 | 50 | 390 | Mo/Ce = 0.034 | Sun et al. (2003) |
| Ru | ng/g | 683 | 5.0 | 0.041 | Ru/Ir = 1.0 | Bézos et al. (2005) |
| Rh | ng/g | 140 | 0.9 | 0.029 | Rh/Ir = 0.7 | Tatsumi et al. (1999) |
| Pd | ng/g | 556 | 3.9 | 0.69 | Pd/Ir = 17 | Bézos et al. (2005) |
| Ag | ng/g | 197 | 8 | 27 | Se/Ag = 7.7 | Hertogen et al. (1980) |
| Cd | ng/g | 680 | 40 | 140 | Cd/Dy = 0.027 | Yi et al. (2000) |
| In | ng/g | 78 | 11 | 75 | In/Y = 0.0025 | Yi et al. (1995) |
| Sn | ng/g | 1680 | 130 | 1000 | Sn/Sm = 0.32 | Jochum et al. (1993) |
| Sb | ng/g | 133 | 5.5 | 14 | Sb/Ce = 0.0012 | Sims et al. (1990) |
| Te | ng/g | 2270 | 12 | 4.9 | $Te/Ni = 2.5 \times 10^{-5}$ | Yi et al. (2000) |
| I | ng/g | 433 | 10 | 21 | $I/K = 1.4\times10^{-5}$ | Deruelle et al. (1992) |
| Xe | mol/g | – | – | $2.1\times10^{-17}$ | molar $He/Xe = 2.6\times10^{7}$ | Sarda and Graham (1990) |
| Cs | ng/g | 188 | 21 | 19 | Rb/Cs = 80 | Hofmann and White (1983) |
| Ba | ng/g | 2410 | 6600 | 16,600 | Log-normal mean of global MORB | This study |
| La | ng/g | 245 | 648 | 3770 | Log-normal mean of global MORB | This study |
| Ce | ng/g | 638 | 1680 | 11,500 | Log-normal mean of global MORB | This study |
| Pr | ng/g | 96.4 | 254 | 1740 | Log-normal mean of global MORB | This study |
| Nd | ng/g | 474 | 1250 | 9800 | Log-normal mean of global MORB | This study |
| Sm | ng/g | 154 | 406 | 3250 | Log-normal mean of global MORB | This study |
| Eu | ng/g | 58.0 | 154 | 1220 | Log-normal mean of global MORB | This study |
| Gd | ng/g | 204 | 544 | 4400 | Log-normal mean of global MORB | This study |
| Tb | ng/g | 37.5 | 99 | 738 | Log-normal mean of global MORB | This study |
| Dy | ng/g | 254 | 674 | 5110 | Log-normal mean of global MORB | This study |
| Ho | ng/g | 56.7 | 149 | 1050 | Log-normal mean of global MORB | This study |
| Er | ng/g | 166 | 438 | 3150 | Log-normal mean of global MORB | This study |
| Tm | ng/g | 25.6 | 68 | 453 | Log-normal mean of global MORB | This study |
| Yb | ng/g | 165 | 441 | 3000 | Log-normal mean of global MORB | This study |
| Lu | ng/g | 25.4 | 67.5 | 454 | Log-normal mean of global MORB | This study |
| Hf | ng/g | 107 | 283 | 2400 | Log-normal mean of global MORB | This study |
| Ta | ng/g | 14.2 | 37 | 224 | Log-normal mean of global MORB | This study |
| W | ng/g | 90.3 | 13[e] | 52.0 | Log-normal mean of global MORB | Arevalo and McDonough (2008) |
| Re | ng/g | 39.5 | 0.28 | 0.83 | $Yb/Re = 3.6\times10^{3}$ | Sun et al. (2003) |
| Os | ng/g | 506 | 3.4 | 0.003 | Re/Os = 300 | Gannoun et al. (2007) |
| Ir | ng/g | 480 | 3.2 | 0.041 | $Ni/Ir = 4.8\times10^{6}$ | Bézos et al. (2005) |
| Pt | ng/g | 982 | 7.1 | 0.45 | Pt/Ir = 11 | Bézos et al. (2005) |
| Au | ng/g | 148 | 1.0 | 1.2 | Au/Ir = 30 | Hertogen et al. (1980); Tatsumi et al. (1999) |

(continued on next page)

**Table 2** (*continued*)

| Element | | CI[a] | SE[b] | MORB | Constraint | Reference(s) |
|---|---|---|---|---|---|---|
| Hg | ng/g | 310 | 10 | 12.6 | $Hg/Mn = 9.6 \times 10^{-6}$ | Salters and Stracke (2004) |
| Tl | ng/g | 143 | 3.5 | 6.6 | Rb/Tl = 230 | Hertogen et al. (1980) |
| Pb | ng/g | 2530 | 150 | 570 | Log-normal mean of global MORB | This study |
| Bi | ng/g | 111 | 2.5 | 9.5 | Bi/Pb = 0.0167 | Salters and Stracke (2004) |
| Th | ng/g | 29.8 | 79.5 | 219 | Log-normal mean of global MORB | This study |
| U | ng/g | 7.80 | 20.3 | 80.0 | Log-normal mean of global MORB | This study |

[a] CI carbonaceous chondrite (CI) values taken from Palme and Jones (2003).
[b] Silicate Earth (SE) values taken from McDonough and Sun (1995), unless otherwise stated.
[c] H abundance in silicate Earth from Palme and O'Neill (2003).
[d] K abundance in silicate Earth from Arevalo et al. (2009).
[e] W abundance in silicate Earth from Arevalo and McDonough (2008).

### 4.2. Log–log concentration correlations

"Canonical" trace element ratios, such as Zr/Hf, Ce/Pb, Nb/Ta, and Th/U remain relatively constant over a large range in concentration and MgO content (Fig. 4) and have commonly been summoned by geochemical studies to constrain terrestrial source compositions, including the DMM (e.g., Salters and Stracke, 2004; Workman and Hart, 2005; Boyet and Carlson, 2006), modern mantle (i.e., DMM + OIB source region; e.g., Hofmann et al., 1986; Newsom et al., 1986), continental crust (e.g., McLennan et al., 1980; Taylor and McLennan, 1985; Sims et al., 1990; Plank and Langmuir, 1998; Rudnick and Gao, 2003), bulk SE (e.g., Jochum et al., 1983; Hofmann, 1988; Sun and McDonough, 1989; McDonough and Sun, 1995; Palme and O'Neill, 2003), and by inference the core (e.g., McDonough, 2003). However, several studies have begun to systematically explore the true constancy and regional variability of some canonical ratios, particularly Nb/U and Ce/Pb (Sims and DePaolo, 1997; Niu et al., 1999; Stracke et al., 2003; Willbold and Stracke, 2006; Pfänder et al., 2007; Sun et al., 2008) and K/U (Arevalo et al., 2009), and found that these ratios are in fact not uniform in the modern mantle and may deviate as a result of asymmetrical partitioning behavior during mantle melting and/or source heterogeneities due to regional differences in the proportion of recycled lithologies. As a result, the true constancy of other commonly cited canonical ratios, and systematic variations in these ratios between different mantle source regions, need to be quantitatively examined to confidently establish the legitimacy of using such proxies as a guide to determining mantle and crustal compositions.

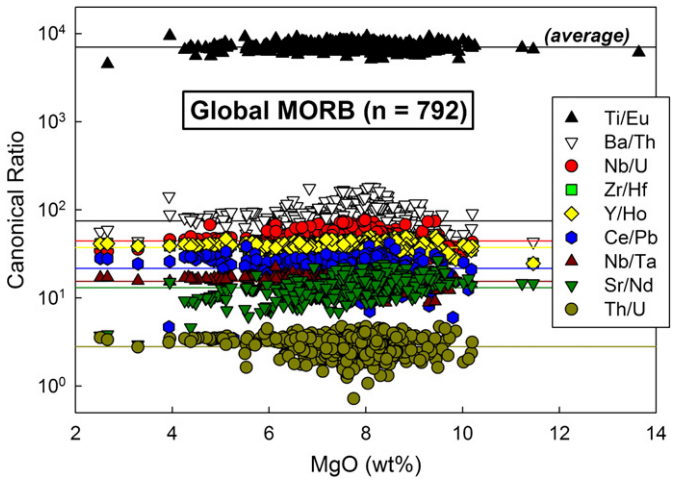


**Fig. 4.** Constancy of "canonical" trace element concentration ratios in global MORB as a function of magmatic processing. Constant trace element ratios are not expected to deviate when plotted versus MgO content, which commonly serves as a proxy for magmatic differentiation. However, log–log covariation diagrams provide a more robust method for determining the relative incompatibility of two elements that behave similarly during geochemical processes. Statistical outliers, defined as data points residing outside of the "outer fence," or 3× the interquartile range, have been excluded.

Historically, the constancy of a canonical trace element ratio was demonstrated by a lack of correlation between the ratio itself (e.g., $i/j$) and the concentration of the elements involved (Jochum et al., 1983; Hofmann et al., 1986; Newsom et al., 1986). However, such comparisons are not statistically robust, as the two variables are not mathematically independent (Sims and DePaolo, 1997). Consequently, errors in the concentration measurement of $i$ (or $j$) appear in both $x$- and $y$-variables. Additionally, variations in $i/j$ are relatively small compared to those in $i$ (or $j$) for any trace element pair with similar partitioning behavior, thus variations in the ratio (typically $<10^1$) pale in comparison to the significantly larger variations seen in concentration (typically $10^1$–$10^3$).

An alternative representation that provides a more robust analysis of the relative incompatibilities of two or more trace elements is a log–log covariation diagram (Sims and DePaolo, 1997; Hofmann, 2003; Willbold and Stracke, 2006; Pfänder et al., 2007; Arevalo and McDonough, 2008; Sun et al., 2008; Arevalo et al., 2009). This type of representation plots statistically independent variables that are dispersed across a wider distribution and a similar order of magnitude along both axes. In this way, the data and their associated errors are weighted uniformly across the range of values.

Solving for $F$, the (modal) accumulated fractional melting equation (Eq. (1)) provides the following relationship between two trace elements in the DMM and a mantle melt such as MORB:

$$\log C_i^{MORB} = \log C_i^{DMM} - \log F + \log\left(1-(1-F)^{1/D_i^{DMM/MORB}}\right) \quad (4)$$

$$\log\left(1-(1-F)^{1/D_i^{DMM/MORB}}\right) = \log C_i^{MORB} - \log C_i^{DMM} + \log F. \quad (5)$$

Therefore, for two elements $i$ and $j$ with equal partition coefficients ($D_i^{sol/liq} = D_j^{sol/liq}$), we arrive at:

$$\log C_i^{MORB} - \log C_i^{DMM} = \log C_j^{MORB} - \log C_j^{DMM} \quad (6)$$

$$\log C_i^{MORB} = \log C_j^{MORB} + \log \frac{C_i^{DMM}}{C_j^{DMM}} \quad (7)$$

which mimics a linear equation in the form $y = mx + b$. Therefore, in the case where elements $i$ and $j$ are equally incompatible ($D_i^{sol/liq} = D_j^{sol/liq}$), the slope ($m$) is equal to unity and the $y$-intercept ($b$) equals the logarithm of the representative $i/j$ ratio of the source.

### 4.3. Effects of mantle source mixing

Although log–log covariation diagrams can and have served as a reliable tool for determining the relative incompatibilities of trace elements during modern mantle melting (Sims and DePaolo, 1997; Hofmann, 2003; Willbold and Stracke, 2006; Pfänder et al., 2007; Arevalo and McDonough, 2008; Sun et al., 2008; Arevalo et al., 2009),

they may also cloud potential source heterogeneities with distinct trace element ratios and/or melting trends. Fig. 5 illustrates how the utility of log–log covariation plots may be compromised by potential mixing (chemical or mechanical) between two or more source components with distinct trace element ratios and partitioning characteristics during melting. As described above, the vast majority (likely >90%) of MORB samples are defined by depletions in highly incompatible elements, such as LILE (e.g., Ba, Th and U), HFSE (e.g., Ti, Zr and Nb) and the light REE (e.g., La, Ce and Pr) compared to less incompatible elements, such as the heavy REE (e.g., Tm, Yb and Lu). Mid-ocean ridge basalts that are characterized by enrichments in highly incompatible elements likely represent mixing between the ambient, depleted component of the DMM and undepleted or enriched mantle domains with distinct trace element attributes.

In an attempt to characterize the K/U ratio of the composite DMM, including both depleted and enriched source components, Arevalo et al. (2009) discretized the K/U ratio measured in N-MORB samples with La/Sm<1.00 (defined by K/U = 20,000 ± 2300, 2σ) and the K/U ratio in E-MORB samples with La/Sm ≥ 1.00 (K/U = 15,700 ± 3100, 2σ). Only considering N-MORB samples, Arevalo et al. (2009) asserted that K and U behave analogously during N-MORB source melting, and thus interpreted that the K/U ratio of global MORB was representative of the composite DMM. Because E-MORB represent a subordinate component of global MORB but are significantly more enriched than N-MORB, these authors modeled a 5% mass contribution of E-MORB and a 6× enrichment relative to N-MORB, resulting in a global MORB and inferred composite DMM K/U ratio of 19,000 ± 2600 (2σ). Fig. 5C, which plots the K and U log abundances of the N-MORB and E-MORB sample sets examined by Arevalo et al. (2009), illustrates the unique slope ($m$) and $y$-intercept ($b$) of E-MORB relative to N-MORB. The deviation in partitioning behavior observed between E-MORB and N-MORB may correspond to distinct source lithologies, a reflection of extremely low degrees of melting (e.g., $F$<0.01) in the case of E-MORB, or mixing between a compositionally depleted and enriched DMM component, such as that which feeds the St. Helena ocean island chain (data from Willbold and Stracke, 2006). Regardless, the partitioning behaviors of K and U are not analogous when considering both N- and E-MORB samples together.

### 4.4. Constancy of canonical trace element ratios

The relative incompatibilities of the trace elements considered here are demonstrated by the log–log covariation diagrams seen in Figs. 6 and 7. In these covariation plots, an equally incompatible pair of elements is distinguished by a linear regression with a slope of unity ($m$ = 1.00); a slope of less than unity ($m$<1.00) indicates a more highly incompatible element along the abscissa ($x$-axis), and a slope of greater than unity ($m$>1.00) reveals a more incompatible element along the ordinate ($y$-axis). Table 3 summarizes the statistics of the linear regressions plotted in Figs. 6 and 7, as well as linear regression

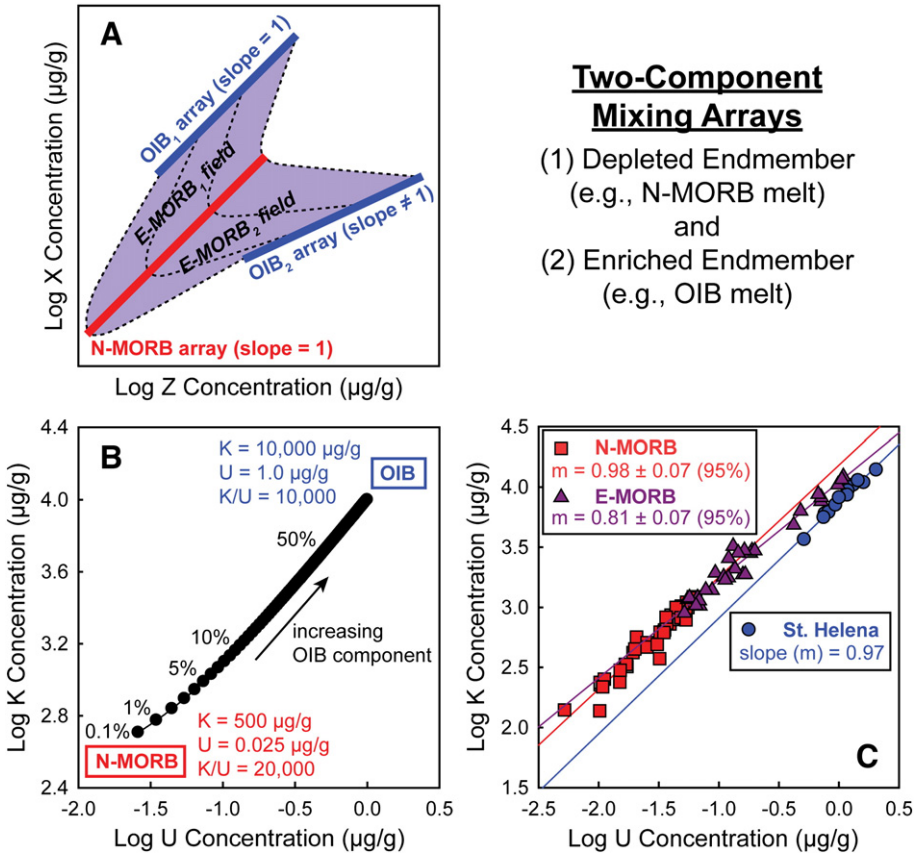


**Fig. 5.** Observable effects of two-component mixing on a log–log covariation diagram. (A) In a log–log covariation plot, an equally incompatible element pair is defined by a linear regression with a slope of unity ($m$ = 1.00), whereas a more incompatible element along the abscissa would be revealed by a slope less than unity ($m$<1.00) and a more incompatible element along the ordinate axis would yield a slope greater than unity ($m$>1.00). Mixing between a depleted and enriched source component could be manifested as an apparent shift in geochemical behavior between two otherwise equally incompatible elements. (B) Two-component mixing between model N-MORB and OIB results in variable K/U ratios as well as K and U abundances. (C) E-MORB samples from Arevalo et al. (2009), which were distinguished by La/Sm ≥ 1.00, could represent two-component mixing between a depleted DMM domain and an enriched mantle domain, such as that which feeds the St. Helena ocean islands (data from Willbold and Stracke, 2006), or a distinct lithology between the depleted component preferentially sampled by N-MORB and the enriched component observed in E-MORB. The samples from Arevalo et al. (2009) suggest that K and U behave analogously during N-MORB genesis but unequally during the genesis of more enriched samples. Interestingly, the K and U abundances from St. Helena OIB hint at equal incompatibility between K and U during melting of this mantle source region.

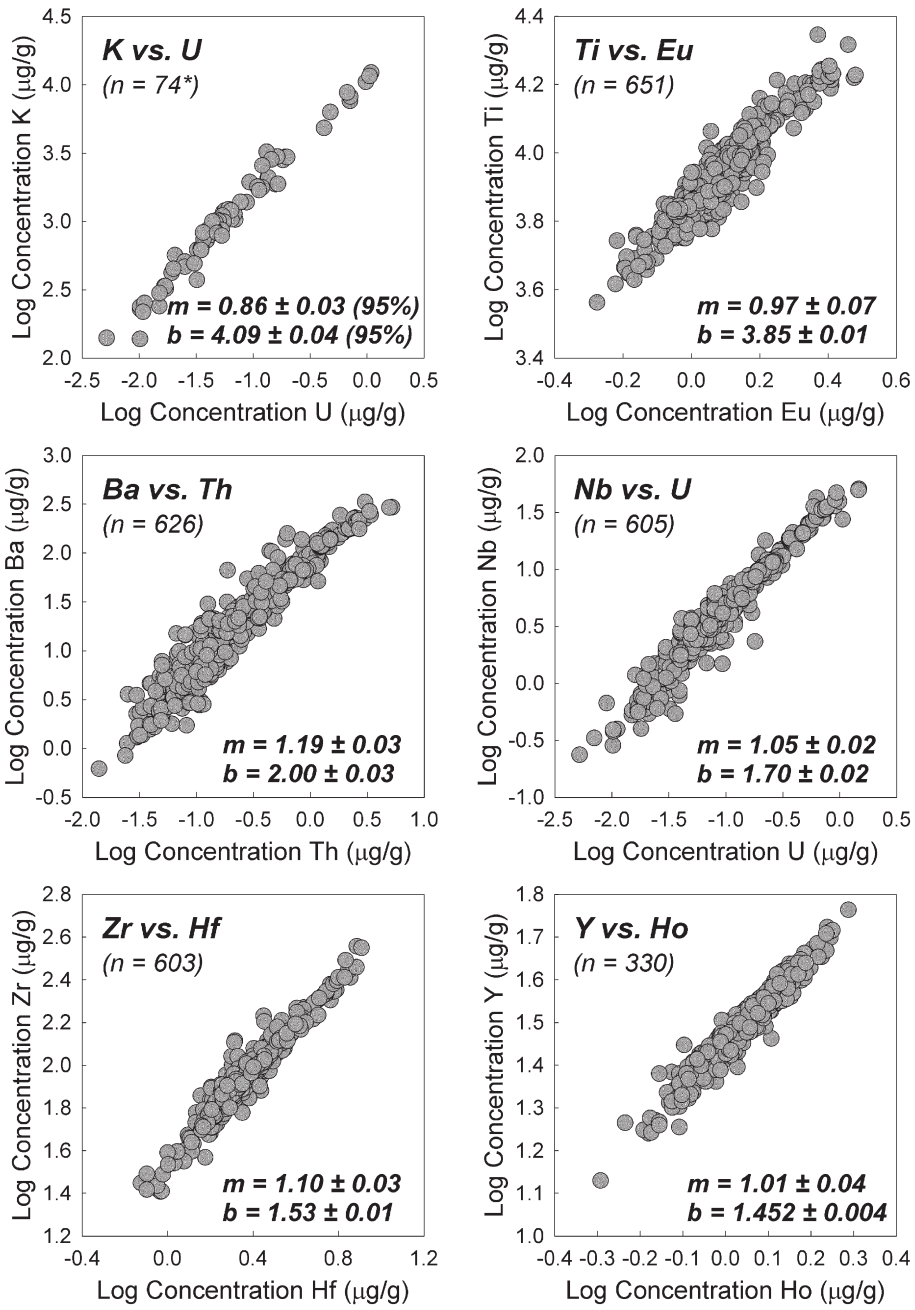


**Fig. 6.** Log–log covariation plots of incompatible trace element pairs. Values for the slopes ($m$) and y-intercepts ($b$), which are given with 95% confidence-limits, are derived from a bivariate linear regression which accounts for uncertainties in both the $x$- and $y$-values unlike traditional univariate regressions (see Supplemental materials). Slopes equal to unity ($m = 1.00$) indicate an equally incompatible pair of trace elements, whereas a slope greater than unity ($m > 1.00$) or less than unity ($m < 1.00$) indicates a more or less, respectively, incompatible element along the ordinate axis. Data for the K vs. U panel were extracted from Arevalo et al. (2009). Statistical outliers, defined by data points residing outside of the "outer fence," or 3× the interquartile range, have been excluded.

statistics considering N-MORB only (samples with $(La/Sm)_N < 1.00$) for comparison.

Our global MORB data set shows that only Ti/Eu ($m = 0.97 \pm 0.07$, 95% confidence-level), Y/Ho ($m = 1.01 \pm 0.04$) and Ce/Pb ($m = 0.97 \pm 0.04$) yield slopes of unity within the uncertainties of the linear regression analyses, trends that are also observed when only considering N-MORB (with the exception of Ce/Pb; see discussion below); thus, these ratios do not statistically fractionate as a function of MORB source melting, mixing or subsequent emplacement and crystallization. Accordingly, the ratios observed in our global MORB database, specifically Ti/Eu = 7060 ± 1270 (2σ), Y/Ho = 28.4 ± 3.6 (2σ) and Ce/Pb = 22.2 ± 9.7 (2σ) may be inferred to represent the composition of the DMM, presuming global MORB adequately represent the compositional heterogeneity, variations in component mixing and melting/crystallization conditions of the DMM (Stracke and Bourdon, 2009). In contrast, Ba/Th, Nb/U, Zr/Hf, Nb/Ta, Sr/Nd, and Th/U yield slopes that are statistically distinct from unity in both global MORB and N-MORB, even within the uncertainties of the linear regression analyses; thus, these canonical trace element ratios fractionate (albeit only slightly for some) during MORB genesis. Interestingly, the behavior of Ce/Pb yields a statistically significant discrepancy when comparing global MORB, which include enriched samples, to N-MORB only. Our global MORB data set suggests that Ce behaves analogously to Pb during MORB genesis, but when

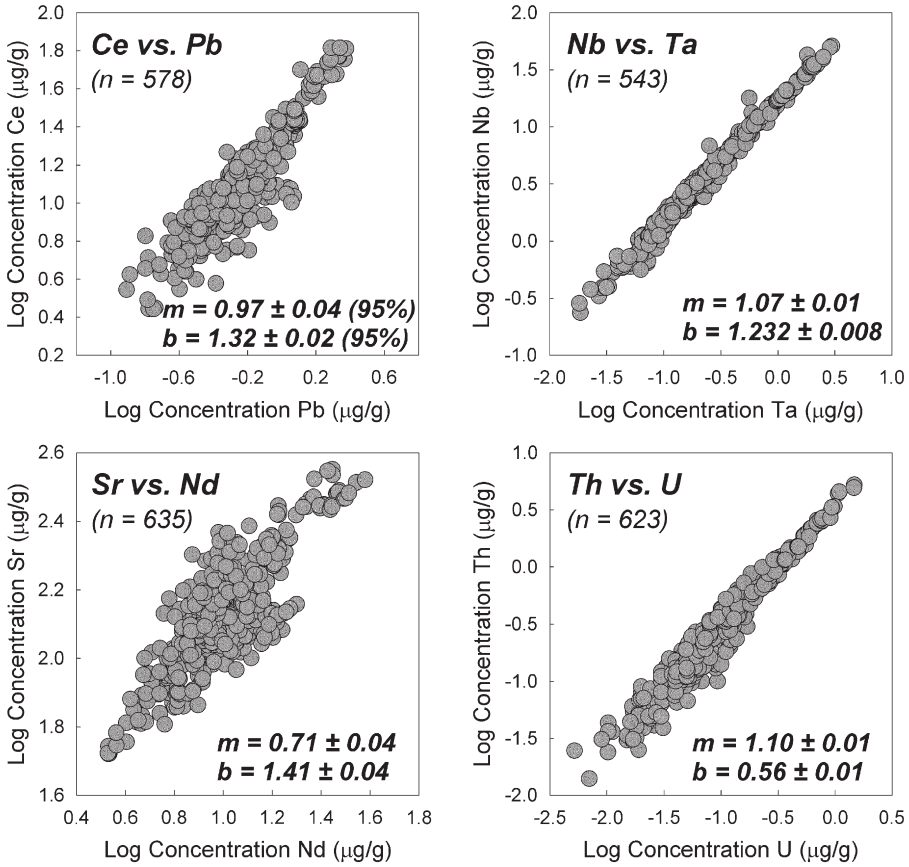


**Fig. 7.** Log–log covariation plots of incompatible trace element pairs (continued).

considering only N-MORB, Pb behaves as a more incompatible element. This result suggests that the enriched component that is observed in global MORB may either: i) have a distinct lithology that partitions Ce and Pb differently than the lithology that dominates the source of depleted MORB samples; ii) be characterized by a distinct Ce/Pb ratio compared to the source of N-MORB, thus equating the discrepancy between global MORB versus N-MORB to different degrees of component mixing; or, iii) represent a different melting or crystallization histories relative to the dominant source component that contributes N-MORB.

## 5. Variations in MORB compositions

### 5.1. Regional distinctions in log-normal mean abundances

Tables 1 and 2 summarize the representative composition of global MORB as determined primarily by the major and trace element chemistry of the comprehensive MORB data set presented here. However, regional geochemical signatures between samples derived from the Atlantic, Indian and Pacific Ocean basins may exist and potentially provide insight into the spatial and/or temporal scale and origin of

**Table 3**
Log–log bivariate linear regression statistics for canonical trace element pairs in global MORB and N-MORB.

| | Ti vs. Eu | Ba vs. Th | Nb vs. U | Zr vs. Hf | Y vs. Ho | Ce vs. Pb | Nb vs. Ta | Sr vs. Nd | Th vs. U |
|---|---|---|---|---|---|---|---|---|---|
| *Global MORB*[a] | | | | | | | | | |
| Slope[b] | 0.97 | 1.19 | 1.05 | 1.10 | 1.01 | 0.97 | 1.07 | 0.71 | 1.10 |
| ±(95% conf) | 0.07 | 0.03 | 0.02 | 0.03 | 0.04 | 0.04 | 0.01 | 0.04 | 0.01 |
| *y*-intercept | 3.849 | 2.00 | 1.70 | 1.53 | 1.452 | 1.32 | 1.232 | 1.41 | 0.56 |
| ±(95% conf) | 0.009 | 0.03 | 0.02 | 0.01 | 0.004 | 0.02 | 0.008 | 0.04 | 0.01 |
| MSWD[c] | 0.15 | 14 | 8.4 | 0.73 | 0.56 | 15 | 3.0 | 2.0 | 8.2 |
| *n* | 651 | 626 | 605 | 603 | 330 | 578 | 543 | 635 | 623 |
| *N-MORB only*[a] | | | | | | | | | |
| Slope[b] | 0.99 | 1.31 | 1.15 | 1.10 | 1.00 | 0.84 | 1.08 | 0.59 | 1.14 |
| ±(95% conf) | 0.10 | 0.06 | 0.05 | 0.03 | 0.05 | 0.06 | 0.02 | 0.05 | 0.04 |
| *y*-intercept | 3.849 | 2.11 | 1.82 | 1.53 | 1.453 | 1.26 | 1.243 | 1.51 | 0.60 |
| ±(95% conf) | 0.010 | 0.05 | 0.06 | 0.01 | 0.004 | 0.02 | 0.015 | 0.05 | 0.04 |
| MSWD[c] | 0.16 | 16 | 9.6 | 0.83 | 0.58 | 16 | 2.9 | 1.8 | 7.0 |
| *n* | 529 | 473 | 452 | 463 | 280 | 431 | 405 | 504 | 469 |

[a] Statistical outliers plotting outside of the "outer fence," defined by 3× the interquartile range, were not considered.
[b] Regressions are derived by minimizing the sum of squares of the distances perpendicular to the best-fit line, following the protocol established in York (1966).
[c] MSWD calculated assuming a uniform uncertainty of ±5% (2σ) for both *x*- and *y*-values.

heterogeneities in the DMM. Geochemical studies have previously established inter-oceanic distinctions based principally on isotopic differences (e.g., Dupré and Allègre, 1983; Allègre et al., 1984; Hart, 1984; Allègre et al., 1987; Ito et al., 1987; Mahoney et al., 1989, 1992; White, 1993; Allègre et al., 1995; Hofmann, 2003 and references therein).

Fig. 8 illustrates the relative enrichment or depletion of MORB samples from each ocean basin with respect to the composition of *all* global MORB. This figure serves to qualitatively illustrate that Atlantic MORB are generally the most enriched in incompatible trace elements, whereas Pacific samples are generally the most depleted, potentially due to the prevalence of slow-spreading ridges in the Atlantic and fast-spreading ridges in the Pacific (e.g., Niu and Hekinian, 1997). Overall, Indian Ocean MORB shows the least variation in incompatible element enrichments/depletions but appear to be depleted in the more compatible elements (e.g., Sc, Ti, Cr, and heavy REE). Table 4 presents the log-normal mean composition of MORB derived from ridge segments from each of the three major ocean basins, as well as *t*-probabilities for each inter-oceanic comparison, representing the probability that MORB samples derived from two different oceanic basins originated from the same mantle source region.

Compared to MORB from the Indian and Pacific Oceans, Atlantic MORB are characterized by the lowest MgO abundances as well as statistically significant (at the ≥95% confidence-level) enrichments in most of the highly incompatible elements, including: Sr, the light REE (i.e., La through Gd), Hf, Pb, Th, U, and the TITAN group elements (i.e., Ti, Ta and Nb). However, the Atlantic samples also show enrichments in the more compatible heavy REE (e.g., Dy, Er and Yb) compared to other MORB. Although these geochemical signatures could be indicative of a distinct Atlantic regional source with a prominent recycled component or different modal proportions of peridotitic minerals (e.g., clinopyroxene due to variable proportions of a pyroxenitic source component; Stracke and Bourdon, 2009), the explanation that most easily accounts for the elevated abundances of both incompatible and compatible elements involves smaller degrees of melting or greater extents of fractional crystallization along the Mid-Atlantic Ridge, due to slow ridge spreading rates in the Atlantic (e.g., Niu and Hekinian, 1997).

Opposite to Atlantic MORB, Pacific samples are distinguished by statistically relevant depletions in highly incompatible Ba, Pb, Th, and U, likely due to greater extents of melting beneath the fast-spreading centers diagnostic of Pacific ridges. Indian samples, on the other hand, show depletions in the more compatible Sc, Ti, Cr, and heavy REE (i.e., from Eu down to Lu); the origin of this geochemical signature may be attributed to a distinct source lithology in the Indian DMM and/or source melting in the garnet field.

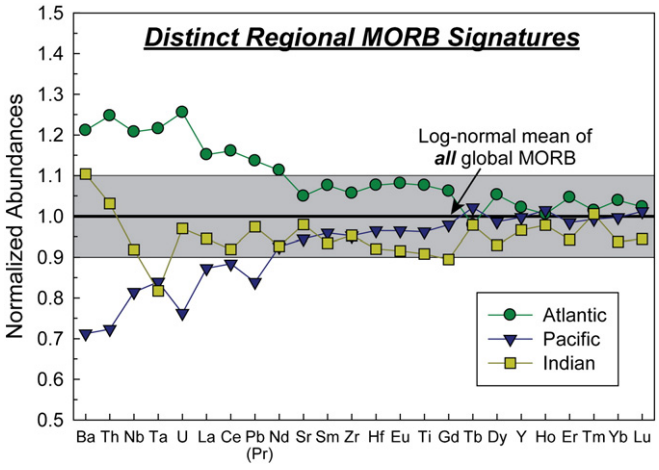


**Fig. 8.** Distinct regional geochemical signatures in trace element abundances of MORB samples derived from the Atlantic, Pacific and Indian Ocean basins. Log-normal mean abundances for MORB from each ocean basin have been normalized to the value measured in *all* global MORB. The shaded field, which represents ±10% deviations from the log-normal mean of the complete global data set, serves to highlight anomalous features, such as the enrichment of incompatible elements (e.g., Ba, Th, U, and light REE) observed in Atlantic MORB compared to samples from the Pacific and Indian Oceans.

### 5.2. Regional variations in canonical trace element ratios

Canonical trace element ratios may also be used to expose regional variations resulting from distinct source compositions, lithologies and mixing/melting/crystallization conditions. For example, Sims and DePaolo (1997) asserted that the average Ce/Pb ratio of Indian Ocean ridge segments was significantly lower than the ratio for Atlantic and Pacific ridges. Sun et al. (2008), however, did not find such a deviation with regard to Ce/Pb, but instead found that the Nb/U ratio of Pacific MORB was distinct from that of Indian and Atlantic samples. As denoted by Sun et al. (2008), such discrepancies between studies may be indicative of distinct DMM source compositions or simply represent sampling biases.

The average, standard deviation and median value of the canonical ratios considered here, which are by and large normally distributed, are given in Table 5 for global MORB as well as sample sets divided by ocean basin. Chondritic ratios and independent *t*-probabilities for each inter-oceanic comparison are also provided. As seen in Table 5, Atlantic MORB are characterized by anomalously low Ti/Eu, Ba/Th, Y/Ho, and Sr/Nd, in addition to distinct Ce/Pb and Th/U ratios relative to Pacific and Indian samples. Because Ti/Eu, Y/Ho and Ce/Pb are conserved during MORB genesis, the distinct ratios identified in Atlantic samples may be inferred to represent distinct source ratios relative to the Pacific and Indian DMM. Conversely, although Ba/Th, Nb/U, Zr/Hf, Nb/Ta, Sr/Nd, and Th/U show some level of statistical distinction between samples derived from Atlantic, Pacific and Indian Ocean ridge segments, these ratios are not preserved during MORB genesis (Figs. 6 and 7); thus, the mantle sources of these basalts cannot be characterized by their respective mantle derivatives, and the distinct ratios exhibited by these samples could reflect variations in mantle source heterogeneity, degrees of component mixing and/or melting/crystallization conditions.

As mentioned above, MORB samples derived from each of the three oceanic basins can be distinguished by their different Th/U ratios, which are statistically distinct at the >99% confidence-level. Statistically distinct Th/U ratios between the Atlantic, Pacific and Indian Ocean basins have been documented before (e.g., Salters and Stracke, 2004) with results similar to those determined here: Indian MORB generally have the highest Th/U ratios (average Th/U = 3.15 ± 0.13, $2\sigma_m$) whereas Pacific samples represent the lowest (Th/U = 2.64 ± 0.09, $2\sigma_m$) despite similar median MgO contents, indicating a counterintuitive decoupling between MgO and Th/U in MORB. Because Th behaves more incompatibly than U, as determined by studies of MORB U–Th disequilibria (e.g., Condomines et al., 1981; Newman et al., 1983; McKenzie, 1985; Goldstein et al., 1989, 1992; Rubin and MacDougall, 1992; Goldstein et al., 1993; Volpe and Goldstein, 1993; Sims et al., 1995), the trace element chemistry of oceanic basalts (e.g., Jochum et al., 1983; Hofmann, 1988; Sun and McDonough, 1989) and the statistical analyses conducted here (Fig. 7), the Th/U ratio of the DMM must be lower than that of its derivatives. As global MORB are characterized by a mean Th/U ratio of 2.87, the global DMM must be characterized by Th/U <2.87, though we find it unlikely that the DMM is characterized by an average Th/U value of ≤2.5, as proposed by some U–Th disequilibria studies (e.g., Condomines et al., 1981; Newman et al., 1983; Goldstein et al., 1989) and models of mantle dynamics (e.g., Jochum et al., 1983; Turcotte et al., 2001). An average DMM Th/U ratio close to 2.5 would provide further evidence for limited Th/U fractionation during crust–mantle differentiation, as both the continental crust (Th/U≈4.3; Rudnick and Gao, 2003) and depleted mantle are only ≤35% different from

**Table 4**
Regional signatures in log-normal trace element abundances measured in MORB.

| | MgO[a] | Sc | Ti | Cr | Sr | Y | Zr | Nb | Ba | La | Ce | Pr | Nd | Sm |
|---|---|---|---|---|---|---|---|---|---|---|---|---|---|---|
| Atlantic MORB | 7.53 | 35.9 | 9150 | 343 | 136 | 30.7 | 95.2 | 4.16 | 20.1 | 4.34 | 13.3 | 1.55 | 10.9 | 3.50 |
| *n* | 310 | 289 | 310 | 53 | 304 | 292 | 304 | 289 | 286 | 315 | 301 | 33 | 299 | 315 |
| Pacific MORB | 8.02 | 39.7 | 8180 | 332 | 123 | 30.0 | 85.8 | 2.81 | 11.8 | 3.29 | 10.2 | 1.75 | 9.03 | 3.12 |
| *n* | 223 | 157 | 219 | 64 | 202 | 189 | 199 | 198 | 215 | 251 | 247 | 205 | 233 | 248 |
| Indian MORB | 8.05 | 33.7 | 7720 | 312 | 127 | 29.0 | 85.9 | 3.16 | 18.3 | 3.56 | 10.6 | 1.78 | 9.04 | 3.04 |
| *n* | 180 | 54 | 150 | 92 | 162 | 169 | 148 | 164 | 183 | 185 | 171 | 134 | 185 | 186 |
| *t-probabilities*[b,c] | | | | | | | | | | | | | | |
| Atlantic vs Pacific | 0.0% | 0.0% | 0.0% | 41% | 0.0% | 24% | 0.4% | 0.0% | 0.0% | 0.0% | 0.0% | 11% | 0.0% | 0.0% |
| Pacific vs Indian | 91% | 0.0% | 1.9% | 4.9% | 24% | 17% | 98% | 20% | 0.0% | 16% | 41% | 64% | 97% | 33% |
| Atlantic vs Indian | 0.0% | 0.3% | 0.0% | 2.2% | 2.1% | 1.0% | 0.9% | 0.3% | 40% | 0.1% | 0.0% | 6.9% | 0.0% | 0.0% |

| | Eu | Gd | Tb | Dy | Ho | Er | Tm | Yb | Lu | Hf | Ta | Pb | Th | U |
|---|---|---|---|---|---|---|---|---|---|---|---|---|---|---|
| Atlantic MORB | 1.32 | 4.67 | 0.722 | 5.38 | 1.06 | 3.30 | 0.460 | 3.11 | 0.464 | 2.58 | 0.272 | 0.647 | 0.273 | 0.100 |
| *n* | 309 | 286 | 63 | 276 | 33 | 274 | 38 | 307 | 299 | 287 | 274 | 270 | 279 | 270 |
| Pacific MORB | 1.18 | 4.31 | 0.754 | 5.04 | 1.07 | 3.10 | 0.450 | 2.99 | 0.459 | 2.31 | 0.188 | 0.478 | 0.158 | 0.061 |
| *n* | 249 | 217 | 220 | 215 | 195 | 216 | 164 | 245 | 233 | 221 | 171 | 173 | 206 | 209 |
| Indian MORB | 1.12 | 3.93 | 0.722 | 4.74 | 1.03 | 2.97 | 0.456 | 2.81 | 0.429 | 2.21 | 0.183 | 0.555 | 0.226 | 0.078 |
| *n* | 171 | 113 | 154 | 154 | 139 | 154 | 104 | 172 | 170 | 160 | 117 | 160 | 163 | 159 |
| *t-probabilities*[b,c] | | | | | | | | | | | | | | |
| Atlantic vs Pacific | 0.0% | 0.1% | 24% | 0.2% | 85% | 0.3% | 59% | 2.4% | 56% | 0.0% | 0.0% | 0.0% | 0.0% | 0.0% |
| Pacific vs Indian | 2.1% | 0.3% | 7.6% | 1.1% | 13% | 5.7% | 66% | 0.3% | 0.1% | 16% | 78% | 0.8% | 0.0% | 0.7% |
| Atlantic vs Indian | 0.0% | 0.0% | 100% | 0.0% | 57% | 0.0% | 84% | 0.0% | 0.0% | 0.0% | 0.0% | 0.2% | 6.0% | 0.6% |

[a] Concentrations are reported in μg/g and represent log-normal means with the exception of MgO, which represents the median and is reported in wt.%.
[b] Statistical outliers plotting outside of the "outer fence," defined by 3× the interquartile range, were not considered.
[c] Student *t*-test probabilities of ≤5% indicate compositions that are statistically distinct at the ≥95% confidence-level.

**Table 5**
Regional signatures in canonical trace element ratios measured in MORB.

| | Ti/Eu[a,b] | Ba/Th | Nb/U | Zr/Hf | Y/Ho[a,b] | Ce/Pb[b] | Nb/Ta | Sr/Nd | Th/U | Eu/Eu*[c] |
|---|---|---|---|---|---|---|---|---|---|---|
| *Atlantic MORB* | | | | | | | | | | |
| Average | 6950 | 75.0 | 43.8 | 36.9 | 27.4 | 22.2 | 15.8 | 12.7 | 2.88 | 1.000 |
| Median | 6950 | 76.5 | 43.7 | 36.9 | 27.3 | 22.1 | 15.8 | 12.3 | 2.92 | 0.998 |
| 2σ | 1130 | 42.3 | 11.2 | 5.8 | 3.7 | 7.8 | 2.6 | 5.6 | 1.07 | 0.105 |
| *n* | 301 | 271 | 269 | 281 | 33 | 270 | 271 | 293 | 270 | 286 |
| $2\sigma_m$ | 65 | 2.6 | 0.7 | 0.3 | 0.6 | 0.5 | 0.2 | 0.3 | 0.07 | 0.006 |
| *Pacific MORB* | | | | | | | | | | |
| Average | 7170 | 81.8 | 47.4 | 37.2 | 28.5 | 23.5 | 15.1 | 13.9 | 2.64 | 0.979 |
| Median | 7140 | 78.0 | 46.6 | 36.9 | 29.3 | 24.8 | 15.4 | 13.9 | 2.54 | 0.973 |
| 2σ | 1330 | 59.9 | 27.6 | 6.7 | 3.8 | 10.8 | 3.2 | 7.3 | 1.26 | 0.129 |
| *n* | 214 | 194 | 183 | 185 | 164 | 173 | 162 | 195 | 198 | 217 |
| $2\sigma_m$ | 91 | 4.3 | 2.0 | 0.5 | 0.3 | 0.8 | 0.3 | 0.5 | 0.09 | 0.009 |
| *Indian MORB* | | | | | | | | | | |
| Average | 7130 | 85.3 | 44.1 | 39.1 | 28.5 | 20.9 | 15.4 | 14.5 | 3.15 | 0.998 |
| Median | 7070 | 80.9 | 45.2 | 39.0 | 28.7 | 20.7 | 15.7 | 14.4 | 3.24 | 0.996 |
| 2σ | 1380 | 59.0 | 17.1 | 7.5 | 3.0 | 10.6 | 3.9 | 6.0 | 1.63 | 0.085 |
| *n* | 136 | 156 | 154 | 136 | 138 | 145 | 107 | 163 | 158 | 112 |
| $2\sigma_m$ | 118 | 4.7 | 1.4 | 0.6 | 0.3 | 0.9 | 0.4 | 0.5 | 0.13 | 0.008 |
| *Global MORB* | | | | | | | | | | |
| Average | 7060 | 79.7 | 45.0 | 37.5 | 28.4 | 22.2 | 15.5 | 13.5 | 2.87 | 0.992 |
| Median | 7030 | 78.3 | 44.3 | 37.2 | 28.7 | 22.3 | 15.7 | 13.2 | 2.89 | 0.991 |
| 2σ | 1270 | 53.3 | 19.2 | 6.8 | 3.6 | 9.7 | 3.2 | 6.5 | 1.35 | 0.112 |
| *n* | 651 | 621 | 606 | 602 | 335 | 588 | 540 | 651 | 626 | 615 |
| $2\sigma_m$ | 50 | 2.1 | 0.8 | 0.3 | 0.2 | 0.4 | 0.1 | 0.3 | 0.05 | 0.005 |
| CI Chondrites[d] | 7900 | 80.8 | 31.7 | 36.1 | 27.5 | 11.2[e] | 17.4 | 15.3 | 3.82 | 1.000 |
| *t-probabilities*[f,g] | | | | | | | | | | |
| Atlantic vs Pacific | 0.0% | 0.7% | 0.1% | 33% | 0.4% | 0.8% | 0.0% | 0.0% | 0.0%0.0% | |
| Pacific vs Indian | 57% | 28% | 0.8% | 0.0% | 88% | 0.0% | 29% | 8.3% | 0.0% | 0.2% |
| Atlantic vs Indian | 0.6% | 0.0% | 73% | 0.0% | 0.4% | 1.2% | 2.3% | 0.0% | 0.0% | 72% |

[a] Trace element ratios characterized by log–log covariation slopes of unity in global MORB.
[b] Trace element ratios characterized by log–log covariation slopes of unity in N-MORB with $(La/Sm)_N < 1.00$.
[c] $Eu/Eu^* = Eu_N/(Gd_N \times Sm_N)0.5$.
[d] CI carbonaceous chondrite ratios taken from Palme and Jones (2003).
[e] Silicate Earth Ce/Pb ratio from McDonough and Sun (1995).
[f] Statistical outliers plotting outside of the "outer fence," defined by 3× the interquartile range, were not considered.
[g] Student *t*-test probabilities of ≤5% indicate compositions that are statistically distinct at the ≥95% confidence-level.

the initial chondritic value (Th/U = 3.82 ± 0.54; Palme and Jones, 2003). The log-normal mean abundances given in Table 4 reveal that the variation in Th/U is a reflection of the variability in both Th and U concentrations observed between MORB from the different oceanic basins.

Global MORB (Eu/Eu* = 0.992 ± 0.005, $2\sigma_m$) do not show a positive Eu anomaly, which would complement the negative Eu/Eu* value observed in the bulk continental crust (Rudnick and Gao, 2003), nor do the divided regional MORB data sets from the Atlantic, Pacific and Indian Oceans despite a range in median MgO values from 7.5 wt.% in the Atlantic (mean Eu/Eu* = 1.000) up to >8.0 wt.% in samples from the Pacific (mean Eu/Eu* = 0.979) and Indian (mean Eu/Eu* = 0.998). In fact, Pacific MORB exemplify a negative Eu/Eu* ratio, indicating a potential decoupling between MgO and Eu/Eu* (which are both associated with plagioclase fractionation) in global MORB. Additionally, the overall lack of a positive Eu anomaly in global MORB, despite a median MgO content of 7.84 wt.%, is counter to what has previously been postulated for relatively primitive MORB (defined by >7.6 wt.% MgO; Niu and O'Hara, 2009).

A complementary way to statistically examine distinct regional geochemical signatures as well as the relative homogenization of the DMM is through the dispersion of the data for each ocean basin. Box-and-whisker plots, such as those shown in Fig. 9, provide a non-parametric, graphical depiction of the statistical scatter associated with a sample population; such representations may be diagnostic of the degree of source heterogeneity, component mixing and/or variation in melting/crystallization conditions of the DMM. Fig. 9 illustrates the dispersion of Ti/Eu, Y/Ho, Nb/Ta and Th/U observed in each of the major ocean basins. Because Ti/Eu and Y/Ho are not fractionated during MORB genesis (and Nb/Ta and Th/U are only fractionated slightly; Fig. 6), the ratios measured in MORB may be inferred to be representative of the DMM. As shown in Fig. 9, Ti/Eu, Y/Ho, Nb/Ta, and Th/U are distinct in most MORB relative to the chondritic value. The enriched Y/Ho and depleted Th/U ratios observed in most global MORB, however, are balanced by the depleted Y/Ho and enriched Th/U ratios found in the continental crust, thus reconciling the silicate Earth (as modeled by the MORB source region + continental crust) with chondrites. Interestingly, Ti/Eu and Nb/Ta are found to be sub-chondritic in both the median of global MORB and the bulk continental crust, requiring an under-represented terrestrial reservoir with a complementary enrichment in Ti and Nb somewhere in the silicate Earth (e.g., refractory, rutile-bearing eclogite at depth in the mantle; McDonough, 1991; Rudnick et al. 2000) or core (e.g., Wade and Wood, 2001).

## 6. Conclusions

We have augmented a set of new, high-precision LA-ICP-MS measurements of global spectrum of MORB samples with a critically compiled collection of analyses from several high-quality, peer-reviewed data sets. From the comprehensive MORB database assembled here, we have developed a compositional model for global MORB as well as N-MORB only (defined by $(La/Sm)_N < 1.00$) for comparison. Additionally, we have statistically evaluated

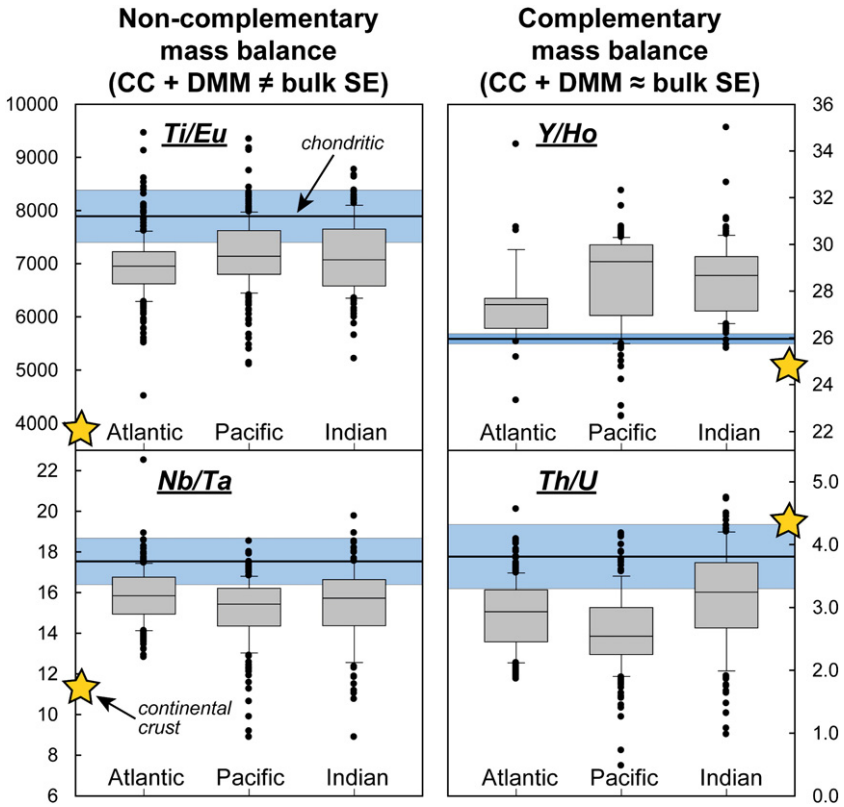


**Fig. 9.** Regional trends and box-and-whisker representations of the data dispersion for several canonical trace element ratios in Atlantic, Pacific and Indian MORB. Box-and-whisker plots provide a non-parametric way of illustrating the degree of statistical dispersion (spread) and skewness in a distribution of data. The lines located near the center of each box represent the median of the data distribution, thereby dividing the data into two equal parts. The edges of the box represent the first and third quartile of the data (also known as the interquartile range), and the whiskers represent the boundary within which 75% of the data reside. Average continental crust (Rudnick and Gao, 2003) is represented by a star (gold). A reference line for carbonaceous chondrites, as modeled by Palme and Jones (2003) for Ti/Eu, Th/U and Nb/Ta, and Pack et al. (2007) for Y/Ho, is represented by a solid line with a shaded (blue) uncertainty field. Global MORB, and by inference the DMM, are largely characterized by super-chondritic Y/Ho and sub-chondritic Th/U ratios; these geochemical signatures are balanced by the bulk continental crust, which is characterized by sub-chondritic Y/Ho and super-chondritic Th/U. However, the bulk continental crust and median global MORB are both characterized sub-chondritic Ti/Eu and Nb/Ta ratios, requiring an under-sampled terrestrial reservoir with a complementary enrichment of Ti/Eu and Nb/Ta, such as refractory, rutile-bearing eclogite (e.g., McDonough, 1991; Rudnick et al., 2000).

the constancy of canonical trace element ratios through MORB genesis and investigated distinct regional geochemical signatures between samples derived from the Atlantic, Pacific and Indian Ocean basins.

Global MORB represent a more incompatible element enriched composition than previously suggested by earlier geochemical models (c.f., Hofmann, 1988; Sun and McDonough, 1989; Su, 2002). Because Ti/Eu (global MORB mean = 7060 ± 1270, 2σ), Y/Ho (28.4 ± 3.6, 2σ) and Ce/Pb (22.2 ± 9.7, 2σ) do not significantly fractionate as a function of MORB genesis (at the 95% confidence-level), the ratios recorded in global (and regional) MORB likely represent the values of the DMM, presuming the source heterogeneity, degree of source component mixing and variations in melting/crystallization conditions of the DMM are adequately represented by the inclusive MORB database compiled here. Alternatively, Ba/Th, Nb/U, Zr/Hf, Nb/Ta, Sr/Nd, and Th/U are all significantly fractionated during MORB genesis and may not be inferred to represent the DMM.

Atlantic MORB are characterized by statistically significant enrichments in the incompatible trace elements, including Sr, the light REE, Hf, Pb, Th, U, and TITAN group elements, as well as enrichments in the more compatible heavy REE (e.g., Dy, Er and Yb); these geochemical attributes, along with the low MgO content associated with Atlantic MORB (median MgO = 7.54 wt.%) compared to Pacific (8.03 wt.% MgO) and Indian MORB (8.05 wt.% MgO), are likely the result of smaller degrees of melting or greater extents of fractional crystallization due to slow ridge spreading rates along the Mid-Atlantic Ridge. Conversely, MORB derived from Pacific spreading centers are generally characterized by the lowest abundances of highly incompatible Ba, Pb, Th, and U, likely due to greater extents of melting beneath the fast-spreading centers diagnostic of Pacific ridges. Indian MORB, on the other hand, exhibit depletions in the more compatible Sc, Ti, Cr, and heavy REE (i.e., from Eu down to Lu), a geochemical signature that may be attributed to a distinct source lithology in the Indian DMM and/or deep source melting in the garnet field. Similar to the continental crust, global MORB and by inference the DMM are defined by sub-chondritic Ti/Eu and Nb/Ta ratios, requiring a complementary Ti- and Nb-rich reservoir somewhere in the silicate Earth (e.g., rutile-bearing eclogite) or core.

## Acknowledgements

We would like to thank Emily Klein, Charles Langmuir, Gaby Loock, Yaoling Niu, Marc Norman, and Michael Perfit, as well as the Division of Petrology and Volcanology, Department of Mineral Sciences, Smithsonian Institute, especially Leslie Hale, Sorena Sorenson and the late Jim Luhr, for assistance acquiring the samples measured in this study. We appreciate analytical support from Richard Ash, statistical insights from Barry Reno, and provocative discussions with Francis Albarède and Albrecht Hofmann. Editorial comments from Andreas Stracke, Albrecht Hofmann and an anonymous reviewer helped to focus this manuscript and are sincerely appreciated. This study was funded by NSF grants #0337621 and #0739006.

## Appendix A. Supplementary data

Supplementary data associated with this article can be found, in the online version, at doi:10.1016/j.chemgeo.2009.12.013.

## References

Ahrens, L.H., 1954. The log-normal distribution of the elements (a fundamental law of geochemistry and its subsidiary). Geochimica et Cosmochimica Acta 5, 49–73.
Allègre, C.J., Turcotte, D.L., 1986. Implications of a two-component marble cake mantle. Nature 323, 123–127.
Allègre, C.J., Hamelin, B., Dupré, B., 1984. Statistical analysis of isotopic ratios in MORB: the mantle blob cluster model and the convective regime of the mantle. Earth and Planetary Science Letters 71, 71–84.
Allègre, C.J., Hamelin, B., Provost, A., Dupré, B., 1987. Topology in isotopic multispace and origin of mantle chemical heterogeneities. Earth and Planetary Science Letters 81, 319–337.
Allègre, C.J., Schiano, P., Lewin, E., 1995. Differences between oceanic basalts by multitrace element ratio topology. Earth and Planetary Science Letters 129, 1–12.
Arevalo Jr., R., McDonough, W.F., 2008. Tungsten geochemistry and implications for understanding the Earth's interior. Earth and Planetary Science Letters 272, 656–665.
Arevalo Jr., R., McDonough, W.F., Luong, M., 2009. The K/U ratio of the silicate Earth: insights into mantle composition, structure and thermal evolution. Earth and Planetary Science Letters 278, 361–369.
Asimow, P.D., Hirschmann, M.M., Stolper, E.M., 1997. An analysis of variations in isentropic melt productivity. Philosophical Transactions of the Royal Society A: Mathematical Physical and Engineering Sciences 355, 255–281.
Bézos, A., Lorand, J.P., Humler, E., Gros, M., 2005. Platinum-group element systematics in mid-oceanic ridge basaltic glasses from the Pacific, Atlantic, and Indian Oceans. Geochimica et Cosmochimica Acta 69, 2613–2627.
Boyet, M., Carlson, R.W., 2006. A new geochemical model for the Earth's mantle inferred from $^{146}Sm$–$^{142}Nd$ systematics. Earth and Planetary Science Letters 250, 254–268.
Condomines, M., Morand, P., Allègre, C.J., 1981. $^{230}Th$–$^{238}U$ radioactive disequilibria in tholeiites from the FAMOUS Zone (Mid-Atlantic Ridge, 36° 50'N): Th and Sr isotopic geochemistry. Earth and Planetary Science Letters 55, 247–256.
Crisp, J.A., 1984. Rates of magma emplacement and volcanic output. Journal of Volcanology and Geothermal Research 20, 177–211.
Davis, A.S., Clague, D.A., Cousens, B.L., Keaten, R., Paduan, J.B., 2008. Geochemistry of basalt from the North Gorda segment of the Gorda Ridge: evolution toward ultraslow spreading ridge lavas due to decreasing magma supply. Geochemistry Geophysics Geosystems 9. doi:10.1029/2007GC001775.
de Argollo, R., Schilling, J.G., 1978. Ge–Si and Ga–Al fractionation in Hawaiian volcanic rocks. Geochimica et Cosmochimica Acta 42, 623–630.
Deruelle, B., Dreibus, G., Jambon, A., 1992. Iodine abundances in oceanic basalts: implications for Earth dynamics. Earth and Planetary Science Letters 108, 217–227.
Donnelly, K.E., Goldstein, S.L., Langmuir, C.H., Spiegelman, M., 2004. Origin of enriched ocean ridge basalts and implications for mantle dynamics. Earth and Planetary Science Letters 226, 347–366.
Dupré, B., Allègre, C.J., 1983. Pb–Sr isotope variation in Indian Ocean basalts and mixing phenomena. Nature 303, 142–146.
Elliott, T., 2003. Tracers of the Slab. In: Eiler, J.M. (Ed.), Inside the Subduction Factory. Geophysical Monograph Series. American Geophysical Union, Washington, DC, pp. 547–568.
Engel, A.E.J., Engel, C.G., Havens, R.G., 1965. Chemical characteristics of oceanic basalts and upper mantle. Geological Society of America Bulletin 76, 719–734.
Gannoun, A., Burton, K.W., Parkinson, I.J., Alard, O., Schiano, P., Thomas, L.E., 2007. The scale and origin of the osmium isotope variations in mid-ocean ridge basalts. Earth and Planetary Science Letters 259, 541–556.
Goldstein, S.J., Murrell, M.T., Janecky, D.R., 1989. Th and U isotopic systematics of basalts from the Juan De Fuca and Gorda Ridges by mass spectrometry. Earth and Planetary Science Letters 96, 134–146.
Goldstein, S.J., Murrell, M.T., Janecky, D.R., Delaney, J.R., Clague, D.A., 1992. Geochronology and petrogenesis of MORB from the Juan De Fuca and Gorda Ridges by $^{238}U$–$^{230}Th$ disequilibrium. Earth and Planetary Science Letters 109, 255–272.
Goldstein, S.J., Murrell, M.T., Williams, R.W., 1993. $^{231}$ Pa and $^{230}Th$ chronology of mid-ocean ridge basalts. Earth and Planetary Science Letters 115, 151–159.
Graham, D.W., Zindler, A., Kurz, M.D., Jenkins, W.J., Batiza, R., Staudigel, H., 1988. He, Pb, Sr and Nd isotope constraints on magma genesis and mantle heterogeneity beneath young Pacific seamounts. Contributions to Mineralogy and Petrology 99, 446–463.
Graham, D.W., Castillo, P.R., Lupton, J.E., Batiza, R., 1996. Correlated He and Sr isotope ratios in south Atlantic near-ridge seamounts and implications for mantle dynamics. Earth and Planetary Science Letters 144, 491–503.
Hall, L.S., Mahoney, J.J., Sinton, J.M., Duncan, R.A., 2006. Spatial and temporal distribution of a C-like asthenospheric component in the Rano Rahi Seamount Field, East Pacific Rise, 15°–19°S. Geochemistry Geophysics Geosystems 7. doi:10.1029/2005GC000994.
Hart, S.R., 1976. Chemical variance in deep ocean basalts. In: Vallier, T.L. (Ed.), Initial Reports of the Deep Sea Drilling Project: National Science Foundation, vol. XXXIV, pp. 301–335.
Hart, S.R., 1984. A large-scale isotope anomaly in the Southern Hemisphere mantle. Nature 309, 753–757.
Hart, S.R., 1993. Equilibration during mantle melting: a fractal tree model. Proceedings of the National Academy of Sciences of the United States of America 90, 11914–11918.
Hertogen, J., Janssens, M.J., Palme, H., 1980. Trace elements in ocean ridge basalt glasses: implications for fractionations during mantle evolution and petrogenesis. Geochimica et Cosmochimica Acta 44, 2125–2143.
Hofmann, A.W., 1988. Chemical differentiation of the Earth: the relationship between mantle, continental crust, and oceanic crust. Earth and Planetary Science Letters 90, 297–314.
Hofmann, A.W., 2003. Sampling mantle heterogeneity through oceanic basalts: isotopes and trace elements. In: R.W. Carlson (Editor), The Mantle and Core. Treatise on Geochemistry Vol. 2 (eds. H.D. Holland and K.K Turekian). Elsevier-Pergamon, Oxford, 61–101.
Hofmann, A.W., White, W.M., 1982. Mantle plumes from ancient oceanic crust. Earth and Planetary Science Letters 57, 421–436.
Hofmann, A.W., White, W.M., 1983. Ba, Rb and Cs in the Earth's mantle. Zeitschrift Fur Naturforschung Section a-a Journal of Physical Sciences 38, 256–266.
Hofmann, A.W., Jochum, K.P., Seufert, M., White, W.M., 1986. Nb and Pb in oceanic basalts: new constraints on mantle evolution. Earth and Planetary Science Letters 79, 33–45.
Ito, E., White, W.M., Gopel, C., 1987. The O, Sr, Nd and Pb isotope geochemistry of MORB. Chemical Geology 62, 157–176.

Iwamori, H., 1993. A model for disequilibrium mantle melting incorporating melt transport by porous and channel flows. Nature 366, 734–737.
Jagoutz, E., Palme, H., Baddenhausen, H., Blum, K., Cendales, M., Dreibus, G., Spettel, B., Lorenz, V., Wanke, H., 1979. The abundances of major, minor and trace elements in the earth's mantle as derived from primitive ultramafic nodules. 10th Proceedings of Lunar and Planetary Sciences, pp. 2031–2050.
Jambon, A., Deruelle, B., Dreibus, G., Pineau, F., 1995. Chlorine and bromine abundance in MORB: the contrasting behaviour of the Mid-Atlantic Ridge and East Pacific Rise and implications for chlorine geodynamic cycle. Chemical Geology 126, 101–117.
Janney, P.E., Le Roex, A.P., Carlson, R.W., 2005. Hafnium isotope and trace element constraints on the nature of mantle heterogeneity beneath the central Southwest Indian Ridge (13°E to 47°E). Journal of Petrology 46, 2427–2464.
Javoy, M., Pineau, F., 1991. The volatiles record of a "popping" rock from the Mid-Atlantic Ridge at 14°N: chemical and isotopic composition of gas trapped in the vesicles. Earth and Planetary Science Letters 107, 598–611.
Jochum, K.P., Hofmann, A.W., Ito, E., Seufert, H.M., White, W.M., 1983. K, U and Th in mid-ocean ridge basalt glasses and heat-production, K/U and K/Rb in the mantle. Nature 306, 431–436.
Jochum, K.P., Hofmann, A.W., Seufert, H.M., 1993. Tin in mantle-derived rocks: constraints on Earth evolution. Geochimica et Cosmochimica Acta 57, 3585–3595.
Jochum, K.P., Dingwell, D.B., Rocholl, A., Stoll, B., Hofmann, A.W., Becker, S., Besmehn, A., Bessette, D., Dietze, H.J., Dulski, P., Erzinger, J., Hellebrand, E., Hoppe, P., Horn, I., Janssens, K., Jenner, G.A., Klein, M., McDonough, W.F., Maetz, M., Mezger, K., Munker, C., Nikogosian, I.K., Pickhardt, C., Raczek, I., Rhede, D., Seufert, H.M., Simakin, S.G., Sobolev, A.V., Spettel, B., Straub, S., Vincze, L., Wallianos, A., Weckwerth, G., Weyer, S., Wolf, D., Zimmer, M., 2000. The preparation and preliminary characterisation of eight geological MPI-DING reference glasses for in-situ microanalysis. Geostandards Newsletter: The Journal of Geostandards and Geoanalysis 24, 87–133.
Jochum, K.P., Willbold, M., Raczek, I., Stoll, B., Herwig, K., 2005a. Chemical characterisation of the USGS reference glasses GSA-1G, GSC-1G, GSD-1G, GSE-1G, BCR-2G, BHVO-2G and BIR-1G using EPMA, ID-TIMS, ID-ICP-MS and LA-ICP-MS. Geostandards and Geoanalytical Research 29, 285–302.
Jochum, K.P., Pfander, J., Woodhead, J.D., Willbold, M., Stoll, B., Herwig, K., Amini, M., Abouchami, W., Hofmann, A.W., 2005b. MPI-DING glasses: new geological reference materials for in situ Pb isotope analysis. Geochemistry Geophysics Geosystems 6.
Johnson, K.T.M., Dick, H.J.B., Shimizu, N., 1990. Melting in the oceanic upper mantle: an ion microprobe study of diopsides in abyssal peridotites. Journal of Geophysical Research: Solid Earth and Planets 95, 2661–2678.
Kelemen, P.B., Hirth, G., Shimizu, N., Spiegelman, M., Dick, H.J.B., 1997. A review of melt migration processes in the adiabatically upwelling mantle beneath oceanic spreading ridges. Philosophical Transactions of the Royal Society A: Mathematical Physical and Engineering Sciences 355, 283–318.
Kinzler, R.J., Grove, T.L., 1992. Primary magmas of mid-ocean ridge basalts: applications. Journal of Geophysical Research: Solid Earth 97, 6907–6926.
Langmuir, C.H., Bender, J.F., Bence, A.E., Hanson, G.N., Taylor, S.R., 1977. Petrogenesis of basalts from the FAMOUS Area: Mid-Atlantic Ridge. Earth and Planetary Science Letters 36, 133–156.
Langmuir, C.H., Bender, J.F., Batiza, R., 1986. Petrological and tectonic segmentation of the East Pacific Rise, 5° 30′–14° 30′N. Nature 322, 422–429.
Laul, J.C., Anders, E., Morgan, J.W., Keays, R.R., Ganapath, R., 1972. Chemical fractionations in meteorites V: volatile and siderophile elements in achondrites and ocean ridge basalts. Geochimica et Cosmochimica Acta 36, 329–345.
le Roex, A.P., Dick, H.J.B., Reid, A.M., Frey, F.A., Erlank, A.J., Hart, S.R., 1985. Petrology and geochemistry of basalts from the American–Antarctic Ridge, Southern Ocean: implications for the westward influence of the Bouvet mantle plume. Contributions to Mineralogy and Petrology 90, 367–380.
le Roux, P.J., Shirey, S.B., Hauri, E.H., Perfit, M.R., Bender, J.F., 2006. The effects of variable sources, processes and contaminants on the composition of northern EPR MORB (8–10°N and 12–14°N): evidence from volatiles ($H_2O$, $CO_2$, S) and halogens (F, Cl). Earth and Planetary Science Letters 251, 209–231.
Lee, C.T.A., Leeman, W.P., Canil, D., Li, Z.X.A., 2005. Similar V/Sc systematics in MORB and arc basalts: implications for the oxygen fugacities of their mantle source regions. Journal of Petrology 46, 2313–2336.
Lundstrom, C.C., Sampson, D.E., Perfit, M.R., Gill, J., Williams, Q., 1999. Insights into mid-ocean ridge basalt petrogenesis: U-series disequilibria from the Siqueiros Transform, Lamont Seamounts, and East Pacific Rise. Journal of Geophysical Research-Solid Earth 104, 13035–13048.
Mahoney, J.J., Natland, J.H., White, W.M., Poreda, R., Bloomer, S.H., Fisher, R.L., Baxter, A.N., 1989. Isotopic and geochemical provinces of the western Indian Ocean spreading centers. Journal of Geophysical Research: Solid Earth and Planets 94, 4033–4052.
Mahoney, J., Leroex, A.P., Peng, Z., Fisher, R.L., Natland, J.H., 1992. Southwestern limits of Indian Ocean ridge mantle and the origin of low $^{206}Pb$–$^{204}Pb$ mid-ocean ridge basalt: isotope systematics of the central Southwest Indian Ridge (17°E–50°E). Journal of Geophysical Research: Solid Earth 97, 19771–19790.
Mahoney, J.J., Graham, D.W., Christie, D.M., Johnson, K.T.M., Hall, L.S., Vonderhaar, D.L., 2002. Between a hotspot and a cold spot: isotopic variation in the Southeast Indian Ridge asthenosphere, 86°E–118°E. Journal of Petrology 43, 1155–1176.
Marty, B., Zimmermann, L., 1999. Volatiles (He, C, N, Ar) in mid-ocean ridge basalts: assessment of shallow-level fractionation and characterization of source composition. Geochimica et Cosmochimica Acta 63, 3619–3633.
McDonough, W.F., 1990. Constraints on the composition of the continental lithospheric mantle. Earth and Planetary Science Letters 101, 1–18.
McDonough, W.F., 1991. Partial melting of subducted oceanic crust and isolation of its residual eclogitic lithology. Philosophical Transactions of the Royal Society of London Series A: Mathematical Physical and Engineering Sciences 335, 407–418.
McDonough, W.F., 1994. Chemical and isotopic systematics of continental lithospheric mantle. In: Meyer, H.O.A., Leonardos, O. (Eds.), Kimberlites, Related Rocks and Mantle Xenoliths. Proceedings of the 5th International Kimberlite conference, vol. 1. CPRM, Brasilia, pp. 478–485.
McDonough, W.F., 2003. Compositional model for the Earth's core. In: R.W. Carlson (Editor), The Mantle and Core. Treatise on Geochemistry Vol. 2 (eds. H.D. Holland and K.K Turekian). Elsevier-Pergamon, Oxford, 547–568.
McDonough, W.F., Frey, F.A., 1989. Rare earth elements in upper mantle rocks. In: Lipin, B.R., McKay, G.A. (Eds.), Geochemistry and Mineralogy of Rare Earth Elements: Reviews in Mineralogy, pp. 99–145.
McDonough, W.F., Sun, S.S., 1995. The composition of the Earth. Chemical Geology 120, 223–253.
McKenzie, D., 1984. The generation and compaction of partially molten rock. Journal of Petrology 25, 713–765.
McKenzie, D., 1985. The extraction of magma from the crust and mantle. Earth and Planetary Science Letters 74, 81–91.
McKenzie, D., Bickle, M.J., 1988. The volume and composition of melt generated by extension of the lithosphere. Journal of Petrology 29, 625–679.
McKenzie, D., O'Nions, R.K., 1991. Partial melt distributions from inversion of rare-earth element concentrations. Journal of Petrology 32, 1021–1091.
McLennan, S.M., Nance, W.B., Taylor, S.R., 1980. Rare earth element-thorium correlations in sedimentary rocks, and the composition of the continental crust. Geochimica et Cosmochimica Acta 44, 1833–1839.
Melson, W.G., Vallier, T., Wright, T.L., Byerly, G., Nelen, J., 1976. Chemical diversity of abyssal volcanic glass erupted along sea-floor spreading centers. Journal Geophysical Research Monograph 19, 351–368.
Michael, P., 1995. Regionally distinctive sources of depleted MORB: evidence from trace elements and $H_2O$. Earth and Planetary Science Letters 131, 301–320.
Morgan, J.W., 1986. Ultramafic xenoliths: clues to Earth's late accretionary history. Journal of Geophysical Research: Solid Earth and Planets 91, 2375–2387.
Nauret, F., Abouchami, W., Galer, S.J.G., Hofmann, A.W., Hemond, C., Chauvel, C., Dyment, J., 2006. Correlated trace element-Pb isotope enrichments in Indian MORB along 18–20°S, Central Indian Ridge. Earth and Planetary Science Letters 245, 137–152.
Newman, S., Finkel, R.C., MacDougall, J.D., 1983. $^{230}Th$–$^{238}U$ disequilibrium systematics in oceanic tholeiites from 21°N on the East Pacific Rise. Earth and Planetary Science Letters 65, 17–33.
Newsom, H.E., White, W.M., Jochum, K.P., Hofmann, A.W., 1986. Siderophile and chalcophile element abundances in oceanic basalts, Pb-isotope evolution and growth of the Earth's core. Earth and Planetary Science Letters 80, 299–313.
Niu, Y.L., 2004. Bulk-rock major and trace element compositions of abyssal peridotites: implications for mantle melting, melt extraction and post-melting processes beneath mid-ocean ridges. Journal of Petrology 45, 2423–2458.
Niu, Y.L., Batiza, R., 1997. Trace element evidence from seamounts for recycled oceanic crust in the eastern Pacific mantle. Earth and Planetary Science Letters 148, 471–483.
Niu, Y.L., Hekinian, R., 1997. Spreading-rate dependence of the extent of mantle melting beneath ocean ridges. Nature 385, 326–329.
Niu, Y.L., O'Hara, M.J., 2009. MORB mantle hosts the missing Eu (Sr, Nb, Ta and Ti) in the continental crust: new perspectives on crustal growth, crust–mantle differentiation and chemical structure of oceanic upper mantle. Lithos 112, 1–17.
Niu, Y.L., Waggoner, D.G., Sinton, J.M., Mahoney, J.J., 1996. Mantle source heterogeneity and melting processes beneath seafloor spreading centers: the East Pacific Rise, 18–19°S. Journal of Geophysical Research: Solid Earth 101, 27711–27733.
Niu, Y.L., Collerson, K.D., Batiza, R., Wendt, J.I., Regelous, M., 1999. Origin of enriched-type mid-ocean ridge basalt at ridges far from mantle plumes: the East Pacific Rise at 11° 20′N. Journal of Geophysical Research: Solid Earth 104, 7067–7087.
Nixon, P.H., Rogers, N.W., Gibson, I.L., Grey, A., 1981. Depleted and fertile mantle xenoliths from southern African kimberlites. Annual Review of Earth and Planetary Sciences 9, 285–309.
Pack, A., Russell, S.S., Shelley, J.M.G., van Zuilen, M., 2007. Geo- and cosmochemistry of the twin elements yttrium and holmium. Geochimica et Cosmochimica Acta 71, 4592–4608.
Palme, H. and Jones, A., 2003. Solar system abundances of the elements. In: A.M. Davis (Editor), Meteorites, Comets, and Planets. Treatise on Geochemistry Vol. 1 (eds. H.D. Holland and K.K Turekian). Elsevier-Pergamon, Oxford, 41–61.
Palme, H. and O'Neill, H.S.C., 2003. Cosmochemical estimates of mantle composition. In: R.W. Carlson (Editor), The Mantle and Core. Treatise on Geochemistry Vol. 2 (eds. H.D. Holland and K.K Turekian). Elsevier-Pergamon, Oxford, 1–38.
Pfänder, J.A., Munker, C., Stracke, A., Mezger, K., 2007. Nb/Ta and Zr/Hf in ocean island basalts: implications for crust–mantle differentiation and the fate of Niobium. Earth and Planetary Science Letters 254, 158–172.
Plank, T., Langmuir, C.H., 1998. The chemical composition of subducting sediment and its consequences for the crust and mantle. Chemical Geology 145, 325–394.
Rubin, K.H., MacDougall, J.D., 1992. Th–Sr isotopic relationships in MORB. Earth and Planetary Science Letters 114, 149–157.
Rudnick, R.L. and Gao, S., 2003. Composition of the continental crust. In: R.L. Rudnick (Editor), The Crust. Treatise on Geochemistry Vol. 3 (eds. H.D. Holland and K.K Turekian). Elsevier-Pergamon, Oxford, 1–64.
Rudnick, R.L., Barth, M., Horn, I., McDonough, W.F., 2000. Rutile-bearing refractory eclogites: missing link between continents and depleted mantle. Science 287, 278–281.
Ryan, J.G., Langmuir, C.H., 1987. The systematics of lithium abundances in young volcanic rocks. Geochimica et Cosmochimica Acta 51, 1727–1741.
Ryan, J.G., Langmuir, C.H., 1988. Beryllium systematics in young volcanic rocks: implications for $^{10}Be$. Geochimica et Cosmochimica Acta 52, 237–244.
Ryan, J.G., Langmuir, C.H., 1993. The systematics of boron abundances in young volcanic rocks. Geochimica et Cosmochimica Acta 57, 1489–1498.

Saal, A.E., Hauri, E.H., Langmuir, C.H., Perfit, M.R., 2002. Vapour undersaturation in primitive mid-ocean-ridge basalt and the volatile content of Earth's upper mantle. Nature 419, 451–455.
Salters, V.J.M., Stracke, A., 2004. Composition of the depleted mantle. Geochemistry Geophysics Geosystems 5. doi:10.1029/2003GC000597.
Sarda, P., Graham, D., 1990. Mid-ocean ridge popping rocks: implications for degassing at ridge crests. Earth and Planetary Science Letters 97, 268–289.
Schilling, J.-G., 1973. Iceland mantle plume: geochemical study of Reykjanes Ridge. Nature 242, 565–571.
Schilling, J.-G., 1991. Fluxes and excess temperatures of mantle plumes inferred from their interaction with migrating mid-ocean ridges. Nature 352, 397–403.
Schilling, J.G., Bergeron, M.B., Evans, R., 1980. Halogens in the mantle beneath the North-Atlantic. Philosophical Transactions of the Royal Society of London Series A: Mathematical Physical and Engineering Sciences 297, 147–178.
Schilling, J.-G., Zajac, M., Evans, R., Johnston, T., White, W., Devine, J.D., Kingsley, R., 1983. Petrologic and geochemical variations along the Mid-Atlantic Ridge from 29°N to 73°N. American Journal of Science 283, 510–586.
Shaw, D.M., 1970. Trace element fractionation during anatexis. Geochimica et Cosmochimica Acta 34, 237–243.
Sims, K.W.W., DePaolo, D.J., 1997. Inferences about mantle magma sources from incompatible element concentration ratios in oceanic basalts. Geochimica et Cosmochimica Acta 61, 765–784.
Sims, K.W.W., Newsom, H.E., Gladney, E.S., 1990. Chemical fractionation during formation of the Earth's core and continental crust: clues from As, Sb, W, and Mo. In: Newsom, H.E., Jones, J.H. (Eds.), Origin of the Earth. Oxford University Press, New York, NY, pp. 291–317.
Sims, K.W.W., Depaolo, D.J., Murrell, M.T., Baldridge, W.S., Goldstein, S.J., Clague, D.A., 1995. Mechanisms of magma generation beneath Hawaii and mid-ocean ridges: uranium/thorium and samarium/neodymium isotopic evidence. Science 267, 508–512.
Sims, K.W.W., Goldstein, S.J., Blichert-Toft, J., Perfit, M.R., Kelemen, P., Fornari, D.J., Michael, P., Murrell, M.T., Hart, S.R., DePaolo, D.J., Layne, G., Ball, L., Jull, M., Bender, J., 2002. Chemical and isotopic constraints on the generation and transport of magma beneath the East Pacific Rise. Geochimica et Cosmochimica Acta 66, 3481–3504.
Sims, K.W.W., Blichert-Toft, J., Fornari, D.J., Perfit, M.R., Goldstein, S.J., Johnson, P., DePaolo, D.J., Hart, S.R., Murrell, P.J., Michael, P.J., Layne, G.D., Ball, L.A., 2003. Aberrant youth: chemical and isotopic constraints on the origin of off-axis lavas from the East Pacific Rise, 9°–10°N. Geochemistry Geophysics Geosystems 4. doi:10.1029/2002GC000443.
Sobolev, A.V., Shimizu, N., 1993. Ultra-depleted primary melt included in an olivine from the Mid-Atlantic Ridge. Nature 363, 151–154.
Spiegelman, M., Kenyon, P., 1992. The requirements for chemical disequilibrium during magma migration. Earth and Planetary Science Letters 109, 611–620.
Stracke, A., Bourdon, B., 2009. The importance of melt extraction for tracing mantle heterogeneity. Geochimica et Cosmochimica Acta 73, 218–238.
Stracke, A., Zindler, A., Salters, V.J.M., McKenzie, D., Blichert-Toft, J., Albarede, F., Gronvold, K., 2003. Theistareykir revisited. Geochemistry Geophysics Geosystems 4.
Su, Y.J., 2002. Mid-ocean ridge basalt trace element systematics: constraints from database management, ICP-MS analyses, global data compilation, and petrologic modeling. Ph.D. Thesis, Columbia University, New York, 457 pp.
Sun, S.-s., Hanson, G.N., 1975. Origin of Ross Island basanitoids and limitations upon heterogeneity of mantle sources for alkali basalts and nephelinites. Contributions to Mineralogy and Petrology 52, 77–106.
Sun, S.-s., McDonough, W.F., 1989. Chemical and isotopic systematics of oceanic basalts: implications for mantle composition and processes. In: Saunders, A.D., Norry, M.J. (Eds.), Magmatism in the Ocean Basins. Geological Society Special Publication, pp. 313–345.
Sun, W.D., Bennett, V.C., Eggins, S.M., Arculus, R.J., Perfit, M.R., 2003. Rhenium systematics in submarine MORB and back-arc basin glasses: laser ablation ICP-MS results. Chemical Geology 196, 259–281.
Sun, W.D., Hu, Y.H., Kamenetsky, V.S., Eggins, S.M., Chen, M., Arculus, R.J., 2008. Constancy of Nb/U in the mantle revisited. Geochimica et Cosmochimica Acta 72, 3542–3549.
Tatsumi, Y., Oguri, K., Shimoda, G., 1999. The behaviour of platinum-group elements during magmatic differentiation in Hawaiian tholeiites. Geochemical Journal 33, 237–247.
Taylor, S.R., McLennan, S.M., 1985. The Continental Crust: Its Composition and Evolution. Blackwell Scientific Publications, Oxford. 312pp.
Taylor, R.N., Thirlwall, M.F., Murton, B.J., Hilton, D.R., Gee, M.A.M., 1997. Isotopic constraints on the influence of the Icelandic plume. Earth and Planetary Science Letters 148, E1–E8.
Turcotte, D.L., Paul, D., White, W.M., 2001. Thorium–uranium systematics require layered mantle convection. Journal of Geophysical Research: Solid Earth 106, 4265–4276.
Volpe, A.M., Goldstein, S.J., 1993. $^{226}Ra$–$^{230}Th$ disequilibrium in axial and off-axis mid-ocean ridge basalts. Geochimica et Cosmochimica Acta 57, 1233–1241.
Wade, J., Wood, B.J., 2001. The Earth's 'missing' niobium may be in the core. Nature 409, 75–78.
White, W.M., 1993. $^{238}U/^{204}Pb$ in MORB and open system evolution of the depleted mantle. Earth and Planetary Science Letters 115, 211–226.
Willbold, M., Stracke, A., 2006. Trace element composition of mantle end-members: implications for recycling of oceanic and upper and lower continental crust. Geochemistry Geophysics Geosystems 7. doi:10.1029/2005GC001005.
Wood, D.A., 1979. Variably veined suboceanic upper mantle: genetic significance for mid-ocean ridge basalts from geochemical evidence. Geology 7, 499–503.
Wood, D.A., Joron, J.L., Treuil, M., Norry, M., Tarney, J., 1979a. Elemental and Sr isotope variations in basic lavas from Iceland and the surrounding ocean floor: nature of mantle source inhomogeneities. Contributions to Mineralogy and Petrology 70, 319–339.
Wood, D.A., Tarney, J., Varet, J., Saunders, A.D., Bougault, H., Joron, J.L., Treuil, M., Cann, J.R., 1979b. Geochemistry of basalts drilled in the North Atlantic by IPOD Leg-49: implications for mantle heterogeneity. Earth and Planetary Science Letters 42, 77–97.
Workman, R.K., Hart, S.R., 2005. Major and trace element composition of the depleted MORB mantle (DMM). Earth and Planetary Science Letters 231, 53–72.
Yi, W., Halliday, A.N., Lee, D.C., Christensen, J.N., 1995. Indium and tin in basalts, sulfides, and the mantle. Geochimica et Cosmochimica Acta 59, 5081–5090.
Yi, W., Halliday, A.N., Alt, J.C., Lee, D.C., Rehkamper, M., Garcia, M.O., Su, Y.J., 2000. Cadmium, indium, tin, tellurium, and sulfur in oceanic basalts: implications for chalcophile element fractionation in the Earth. Journal of Geophysical Research: Solid Earth 105, 18927–18948.
York, D., 1966. Least-squares fitting of a straight line. Canadian Journal of Physics 44, 1079–1086.
Zindler, A., Staudigel, H., Batiza, R., 1984. Isotope and trace element geochemistry of young Pacific seamounts: implications for the scale of upper mantle heterogeneity. Earth and Planetary Science Letters 70, 175–195.